High Lift-over-Drag Earth Re-entry

Executive Summary

Document No.:	**HL-OHB-ES**		
Issue:	**1**	Issue Date:	20.04.2009
Revision:	**1**	Revision Date:	10.08.2009
DIL Reference:	**TBD**		
CI-number	**N/A**		

Document Information:

WP No.:	WP 6000		
SW Tool:	Microsoft Word (Office 2003)	Total Pages:	54

Action	Name / Signature	Company	Date
Prepared by:	M. Tausche	OHB-System	20.04.2009
Checked by:	R. Janovsky	OHB-System	20.04.2009
Product Assurance:			
Authorised by:	M. Tausche	OHB-System	20.04.2009
Accepted by:	R. Molina	ESA	

DOCUMENT CHANGE RECORD

Issue	Date	Affected Pages or Section / Amendment / Correction
1	17.04.2009	Initial Issue
1 Revision 1	10.08.2009	Page 1: Removal of Copyright (Schutzvermerk)

TABLE OF CONTENTS

1 INTRODUCTION AND OUTLINE 4

2 EARTH RE-ENRY STRATEGIES 5

2.1 State-of-the-Art Re-entry Strategies 5

2.2 Innovative Re-entry Strategies 8

3 TYPICAL MISSIONS & PARAMETERS FOR EARTH ENTRY 21

3.1 Low Earth Orbit (LEO) 21

3.2 Moon 22

3.3 Mars 29

4 LAUNCH AND LANDING SITES FOR A HIGH L/D VEHICLE 30

4.1 Preferred Launch Sites 30

4.2 Preferred Landing Sites 31

5 REFERENCE CONFIGURATION OF A HIGH L/D VEHICLE FOR EARTH RE-ENTRY 34

5.1 Reference Vehicle 34

5.2 System Performance 36

6 GUIDANCE PERFORMANCES FOR A HIGH L/D VEHICLE 45

6.1 Guidance And Control 45

6.2 Navigation 49

7 STUDY SYNTHESIS & RECOMMENDATIONS 51

7.1 Study Synthesis 51

7.2 Recommendations for Next steps 52

8 LITERATURE AND ABBREVIATIONS 53

8.1 Applicaple Documents 53

8.2 Reference Documents 53

8.3 Acronyms and Abbreviations 54

1 INTRODUCTION AND OUTLINE

The interest of European and International Space Nations, of human transport from LEO (ISS) and exploration missions, leads to the focus on safe and comfortable earth re-entry with superorbital speeds, for nominal and emergency return with a large variety of possible landing sites. Several re-entry strategies are feasible – from classical, direct capsule re-entry over a skip re-entry to aerocapture/aerobraking with the following orbital re-entry. But to achieve the objectives mentioned above, vehicles with a high lift-to-drag (L/D) ratio are necessary.

The study identifies the potential benefits by using a vehicle with a hypersonic L/D higher than 1.2.

It starts with a description of already existing or innovative entry strategies, the typical missions and parameters for this study are described followed by the selection of the Launch – and Landing sites. After that a comparison of potential vehicles will be shown with the reference re-entry aerodynamic and aerothermodynamic as well as the flight mechanics and guidance strategies which identify the potential benefits of such vehicles.

Finally the necessary next steps will be recommended.

All detailed descriptions elaborated in this study are described in the following Technical Notes:

TN-4.1: Literature Survey of guidance Techniques for Earth Re-entry for Human Mission

TN-4.2: Appraisal of entry techniques for the Earth re-entry of high L/D Vehicles

TN-4.3: Preliminary Reference Configurations

TN-4.4-1: Re-entry Mission Analysis

TN-4.4-2: Guidance Techniques for Earth Re-Entry for Human Missions

TN-4.5: Entry Guidance Performance Verification

TN-4.6: Synthesis & Recommendations

2 EARTH RE-ENRY STRATEGIES

2.1 STATE-OF-THE-ART RE-ENTRY STRATEGIES

The main difference between the earth re-entry strategies of different vehicle types is how far the vehicle travels from the point it first encounters the atmosphere to the point where it lands. This distance is predominantly dictated by how much lift the spacecraft generates while it travels through the atmosphere.

2.1.1 Ballistic strategy (capsule)

Capsules returning to Earth follow conventionally a ballistic entry trajectory. In this case, the vehicle generates low aerodynamic lift which results in a relatively low lift-to-drag (L/D) ratio (about 0.3). The vehicle plunges into the atmosphere and its trajectory is mainly determined by influence of gravity and drag. The landing point is predetermined by the entry conditions and there is little control over the capsule's trajectory or its landing point. Since the vehicle essentially falls vertically through the atmosphere, its downrange distance or ground track is relatively small. Russian Soyuz capsules currently use ballistic entry paths today (see Figure 2-1 and Figure 2-2).

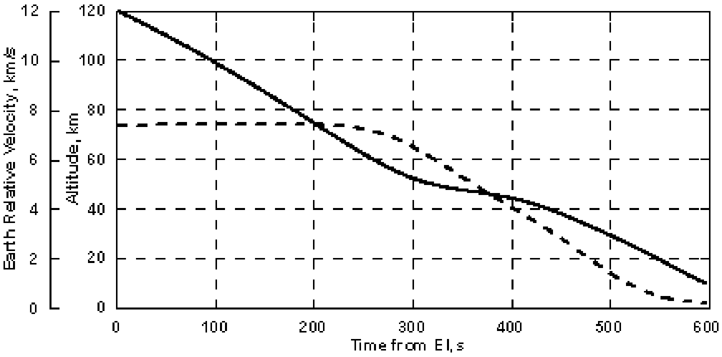

Figure 2-1: Nominal Soyuz Re-entry Trajectory

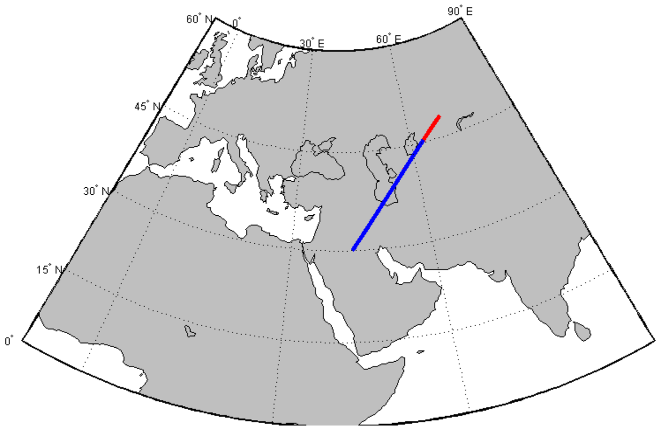

Figure 2-2: Soyuz Groundtrack (ballistic re-entry)

2.1.2 Skip Re-entry (capsule)

A different re-entry option for capsules at super-circular velocities (e.g. from Moon) is the skip entry trajectory. The only option under consideration (e.g. by ORION, see Figure 2-3 and Figure 2-4) is a one skip procedure, where the vehicle enters the atmosphere at super-orbital speeds and decelerates by the aerodynamic drag. At the same time, the vehicle also generates and uses the lift to pitch up and leave the atmosphere. After the first skip the vehicle reaches the LEO speed and can re-enter along an almost ballistic path to touchdown. The attraction of the skip trajectory is that the vehicle can travel with much more downrange in comparison to the semi-ballistic option. The main disadvantage is the significantly higher aerothermodynamic heat loads due to the multiple passes through the atmosphere and the associated longer re-entry duration.

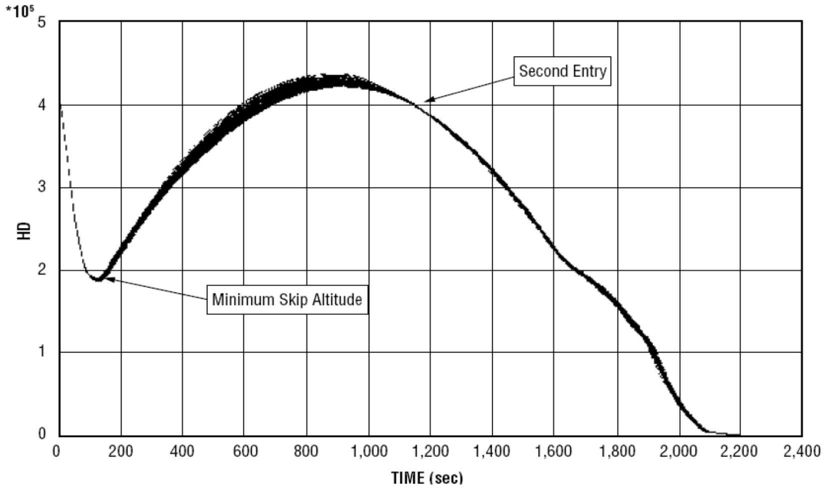

Figure 2-3: Altitude versus time for CEV skip re-entry

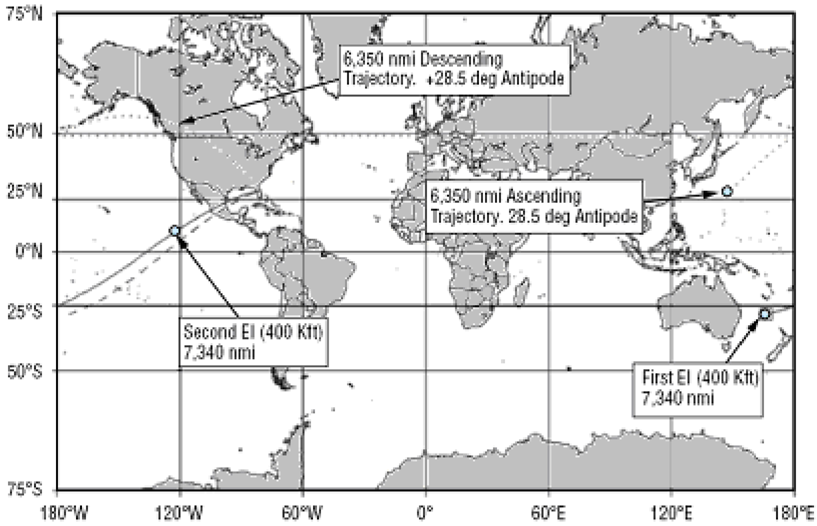

Figure 2-4: Ground track for CEV skip re-entry

2.1.3 Glide trajectory (SpaceShuttle)

An alternative re-entry approach is the glide trajectory (Figure 2-5 and Figure 2-6) in which the vehicle flies through the atmosphere comparable to an aircraft. The spacecraft (e.g. the Space Shuttle) enters the atmosphere with a high angle of attack to generate aerodynamic lift. In this case, the vehicle has a lift-over-drag ratio of about one, which allows travelling with larger downrange than a ballistic - or skip re-entry strategy. The main advantage of this technique is, that there is more control over the vehicle's trajectory and it is possible to choose the several landing site. A further advantage is, that the vehicle would typically lands on a runway and can be reused again. The Space Shuttle typically re-enters with an angle of attack of about 40° to sufficiently slow down the vehicle at the early phase of the re-entry path. This is quite high and making the first trajectory leg of a gliding re-entry similar to a ballistic re-entry, with little control over the trajectory and posing evident safety issues.

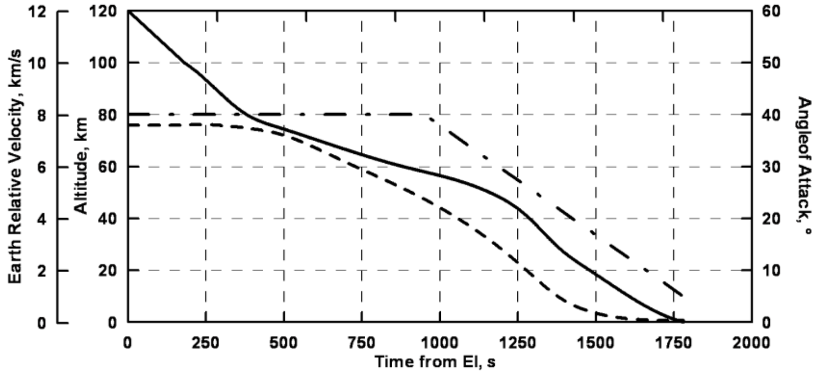

Figure 2-5: Space Shuttle Nominal Trajectory

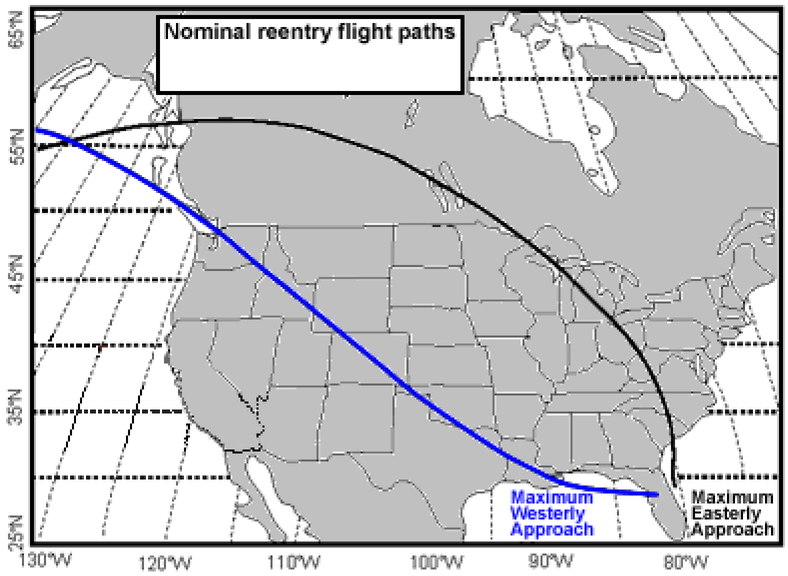

Figure 2-6: Possible Ground tracks for Space Shuttle Nominal Re-entry

2.1.4 SYNTHESIS OF STATE-OF-THE-ART RE-ENTRY STRATEGIES

The different performances for the re-entry strategies existing or under development are presented in Table 2-1. The Table summarizes the peak decelerations and heat fluxes experienced during the different re-entry trajectories.
The radiative heat flux refers to the heat flux from the high temperature air enveloping the capsules. Due to the large radius of curvature of these vehicles the air cap is very thick and, consequently the amount of heat radiated by air in the stand-off distance and impinging on the front part of the capsule is comparable and even larger than the convective heat flux.
The data for the ORION (CEV) direct re-entry are similar to the Apollo CM, since the re-entry strategies are very similar. As can be noted, lifting trajectories (in particular those making use of "skip" strategies) present advantages over the other existing re-entry strategies in terms of both mechanical and aerothermal maximum loads.

Reentry Vehicle	Strategy	Max deceleration, g	Max heat flux, MW/m^2	Radiative heat flux MW/m^2
Soyuz (LEO)	Ballistic	9	0.75	Very low
Soyuz (LEO)	Lifting	3.1	0.65	Very low
CEV(ISS)	Lifting	3	0.32	Very low
Shuttle Orbiter (ISS)	Lifting	2	0.57	Very low
Zond (MOON)	Ballistic	15.8	3	5.1
Zond (MOON)	Lifting	7.8	2.6	4.7
Apollo (MOON)	Lifting	8	2.2	4.7
CEV(MOON)	Lifting (skip reentry)	4	1.3	4.2
CEV(MOON)	Lifting (direct reentry)	6.5	1.7	4.5

Table 2-1 Comparison of different vehicles trajectory parameters for conventional re-entry

2.2 INNOVATIVE RE-ENTRY STRATEGIES

Innovative (airplane-like) re-entry vehicles have been proposed for earth re-entry that relies on the exploitation of lift forces to accomplish a less risky flight through the higher atmosphere. The most important characteristic of these vehicles is the influence of the lift force that implies a large value of Lift-over-Drag (L/D) and at the same time a large manoeuvring ability, i.e. a large L/m ratio or a small wing loading m/S. It is appropriate here to recall that high L/D is achieved not only by the aerodynamic design (e.g. by winged vehicles with sharp fuselage tips and wing leading edges) but also by flying at relatively small angles of attack. Small wing loading (in the order of 1/4 of the Space Shuttle) and small angle of attack (in the order of 1/2 of the Shuttle) justifies the innovative character of the vehicle and of the re-entry strategy. In particular:

1) the winged vehicle has a relatively low wing loading (< 100 Kg/m^2) which is possible by a relatively low structural mass (hot structure concept) and a large wing surface area. As a consequence, the re-entry corridor shifts towards much higher altitudes and the vehicle takes advantage of the lift force to be aerodynamically controlled and decelerated in a more rarefied atmosphere by reducing peak decelerations and heat fluxes. The re-entry trajectory is characterized by longer re-entry times and larger down- and crossranges.

2) The vehicle design is characterized by relatively sharp leading edges of the fuselage and of the wings. During re-entry, the vehicle is aerodynamically controlled by modu-

lating lift and drag forces. Due to the relatively low angles of attack during the flight at high altitudes, the Lift over Drag ratio is relatively high (in the order of two). High heat fluxes are localized at the fuselage - and wing leading edges while heat loads on the belly side of the vehicle surface are reduced.

Re-entry strategies for these high L/D -, low m/S vehicles, exploiting new concepts of lift modulation and long duration flight. The corridor boundaries are imposed by the requirements dictated by the vehicle structure integrity and by the crew survival, including the maximum allowable deceleration. The corridor boundaries include:

1) the equilibrium glide boundary for aerodynamic control after capture within the atmosphere (blue curve in Figure 2-7); it is the upper equilibrium glide curve corresponding to a constant flight path angle at a prescribed value of the lift-coefficient

2) the aerodynamic heating boundary (red curve in Figure 2-7); it is the curve corresponding to the maximum radiation equilibrium temperature at the stagnation point that the tip material can tolerate (radiation equilibrium temperatures about 2450K). Such temperatures can be tolerated only by innovative Ultra High Temperature Ceramic Materials (UHTC) at the nose tip and at the wing leading edges.

3) the curve corresponding to the maximum deceleration (green curve in Figure 2-7) .

In order to identify the solution for the vehicle structure/configuration/operation and for the mission and system design it must be started with the most critical requirement, which is the integrity of the re-entry vehicle at the most severe aerothermal conditions. This means that some UHTC material must be available, that can withstand a high equilibrium radiative temperature at the stagnation point (in the order of 2500K)

For spaceplane-like re-entry vehicles flying at small angle of attack (AoA<20), considering 1g-limit deceleration, the corridor is defined by the yellow area in Figure 2-7. The limit of 1g has been considered because the proposed re-entry strategy implies very low deceleration. Higher deceleration limits (e.g. 7 g as prescribed in CEV requirements) correspond to curves below the thermal boundary curve.

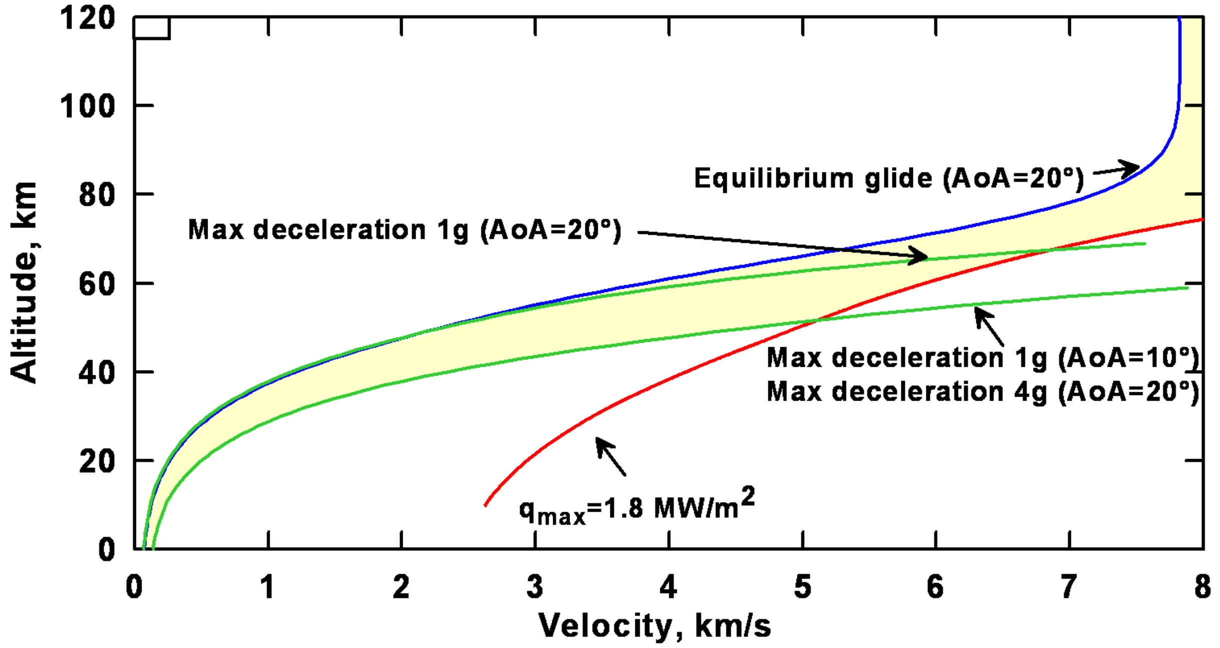

Figure 2-7: Entry corridor

In this case, the upper and lower boundaries of the entry corridor correspond to two completely different re-entry strategies that will be presented in detail in the following.

The initial conditions are: altitude 120 km; Inertial velocity 7.8 km/s; flight path angle -1°. The first approach leg is the same for both trajectories. Indeed, it corresponds to an approach leg with the vehicle flying at an angle of attack equal to 20° and zero bank angle. Before the upper boundary of the entry corridor is encountered (at an altitude of approximately 75 Km) one or another trajectory can be followed by proper AoA/AoB modulation. In the present case of re-entry from LEO aerodynamic force modulation has been accomplished by angle of attack (pitch) modulation only, keeping constant bank angle (AoB=0).

For the high L/D vehicles we choose the velocity-altitude representation (instead of deceleration/velocity) because we can refer to two flight parameters that can be measured instantaneously and accurately.

To minimize heat fluxes, the best trajectory is to use the one at the maximum possible altitude (upper boundary trajectory). This trajectory is composed by the first leg at constant altitude and a second leg corresponding to the maximum lift coefficient. The lower boundary of the entry corridor includes a first leg at constant heat flux (the maximum tolerable) and a second leg at constant maximum deceleration.

Other possible gliding re-entry trajectories are possible within the entry corridor. For instance it is possible to move along a trajectory at constant heat flux less than the maximum heat flux, leaving the upper boundary (red dashed leg in Figure 2-8). On the other and it is possible to move along a trajectory at constant altitude, leaving the lower boundary (black leg in Figure 2-8).

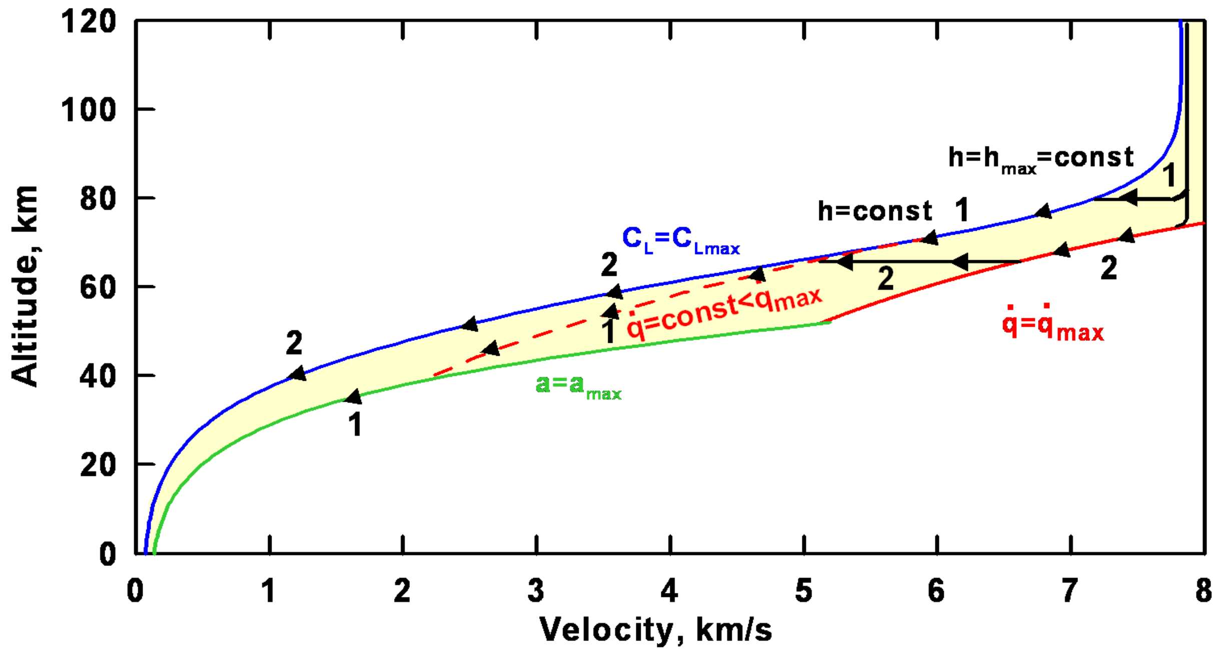

Figure 2-8: Possible re-entry trajectories

2.2.1 EQUILIBRIUM GLIDE RE-ENTRY

Using lift modulation a constant altitude flight is achieved in the first part of the trajectory.

When the equilibrium upper boundary (equilibrium glide, see Figure 2-7) is encountered, corresponding to the quasi-level flight at very small flight path angle with the maximum lift coefficient. The angle of attack should be kept fixed at its maximum value, in order to follow the upper boundary of the entry corridor. In the latter case, the peak heating decreases with the velocity with a third power law, the deceleration decreases with a quadratic power law, and the flight duration (and correspondingly the downrange) is the maximum possible.

Note: This trajectory imposes higher lift to fly at higher altitude and the angle of attack is in average higher than along the lower boundary trajectory.

2.2.2 CONSTANT STAGNATION POINT HEAT FLUX RE-ENTRY

The technological solution found for the TPS dictates the requirements of the trajectory. If the TPS can withstand the maximum radiative equilibrium temperature at the stagnation point it would be desirable to limit the re-entry duration and the crew cabin overheating by imposing a “constant heat flux” trajectory. This trajectory can be implemented by proper aerodynamic force modulation using pitch modulation. In the present case the angle of attack has been modulated with zero bank angle for the entire re-entry trajectory. At sufficiently low altitude, when the velocity is lower, the lower boundary of the re-entry corridor is mainly driven by the maximum deceleration requirement (e.g. 1 g-limit corresponding to AoA=10°).

As shown by Figure 2-9 to Figure 2-10, this trajectory (referred to as “lower boundary” trajectory) has a total duration of approximately 2500 s. The maximum heat flux at the stagnation point of 1.8 MW/m^2 is dictated by the TPS requirement. During the vehicle descent, this boundary is encountered after approximately 500 s. After this time, the AoA is modulated in such a way that the heat flux is held constant until t=1800s. The angle of attack is initially reduced from 20° until 7.5° and then it is properly modulated. At t=1800s the vehicle reaches the altitude and velocity corresponding to the maximum deceleration boundary so that modulation terminates and re-entry continues along the lower boundary of the entry corridor with the angle of attack held constant.

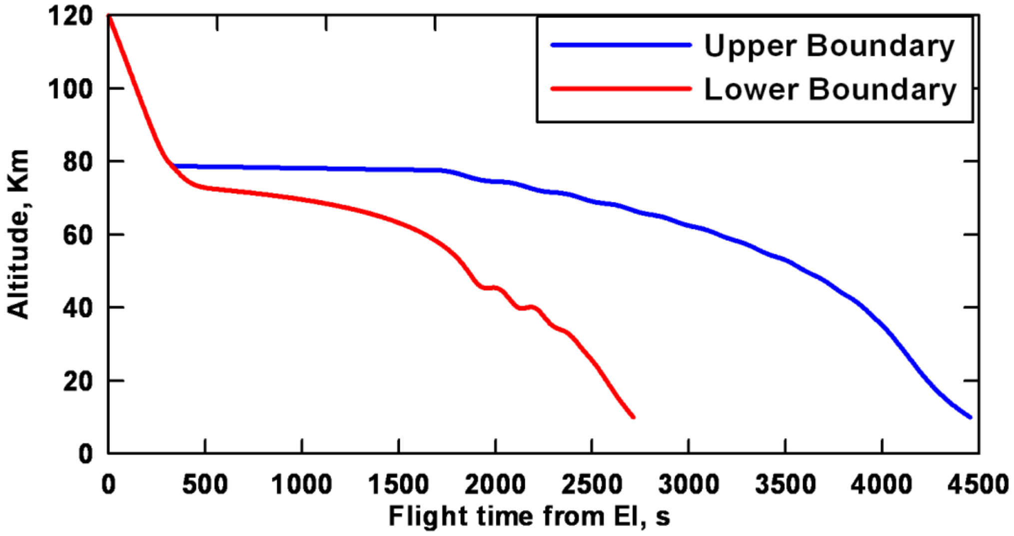

Figure 2-9: Altitude versus time

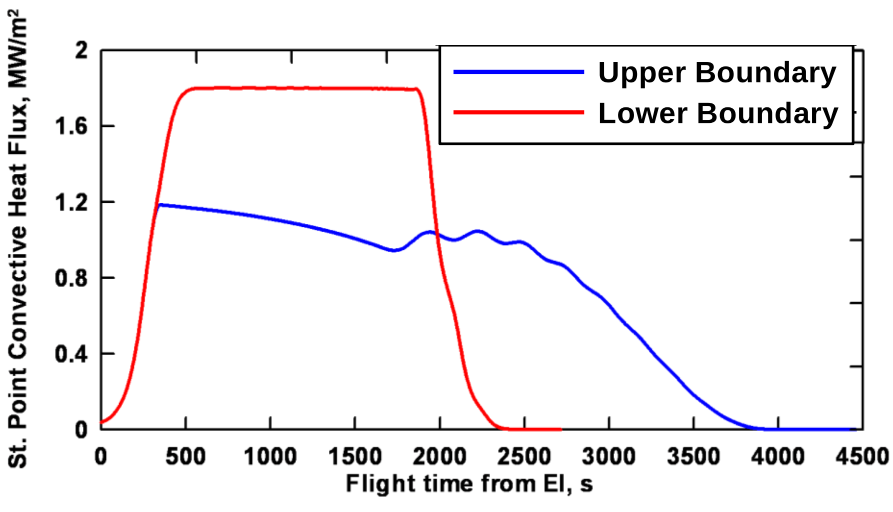

Figure 2-10: Heat flux versus time

2.2.3 COMPARISON BETWEEN DIFFERENT INNOVATIVE RE-ENTRY STRATEGIES

A comparison of the performances, in terms of downrange and crossrange, is shown in Figure 2-11. In addition to the already discussed upper and lower boundary trajectories, obtained for zero bank angle, the cross-ranges have been evaluated considering a different modulation of the AoA up to the maximum value of 20°, with a constant bank angle of AoB=0°and AoB=45. It is evident that increasing the bank angle the entry time and the downrange are reduced and the cross range increases. Of course to increase the bank angle one has to increase the angle of attack in order to increase the total lift and this could be not convenient due to larger heat fluxes on the belly side.

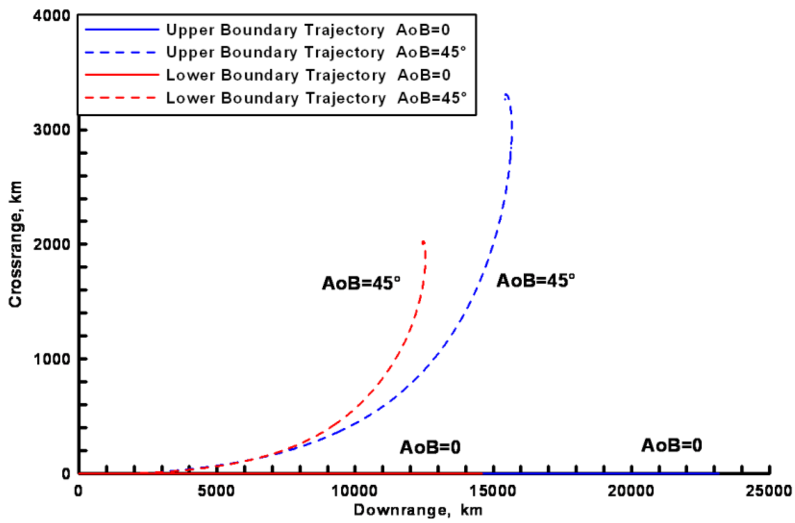

Figure 2-11: Crossrange vs Downrange for the upper and lower trajectories

The idea of exploiting the lift forces also for re-entry beyond LEO is of particular interest when considering that for these high L/D vehicles. Lift forces can help reducing the deceleration peaks and limiting the heat fluxes by allowing the airplane to fly at the maximum possible altitudes (upper boundary trajectory). Returning from exploration missions mean velocities at entry interface (EI) above 8 Km/s (e.g. about 11Km/s for re-entry from Moon) and subsequently much higher kinetic energy must be converted into thermal energy (high decelerations and high heat fluxes) that would be dangerous for the structure integrity and for the crew survival.

The re-entry strategies from exploration missions are not significantly different in principle in comparison to the re-entry logics from LEO. Upper boundary and lower boundary trajectories (glide and constant heat flux, respectively) can be carried out by proper aerodynamic force modulation, using pitch or bank modulation. In this case lift modulation has been accomplished either by angle of attack or by bank modulation and, in some cases, with a mixed control (angle of attack plus bank modulation) due to higher velocities and the resulting higher heat fluxes.

This means for the equilibrium glide re-entry: To minimize heat fluxes one should follow a re-entry trajectory at the maximum possible altitude. Once the super-orbital branch of the equilibrium glide boundary is encountered, corresponding to the quasi-level flight at very small flight path angle with the maximum lift coefficient (AoA=45°), using lift modulation by pitch and/or bank modulation, a constant altitude flight (at an altitude of about 85 Km) can be achieved. Since the velocity is super-orbital a negative lift is initially required in order to balance the centrifugal force (vehicle in lift-down attitude). During the constant altitude flight the lift is reduced until zero and then, after the orbital speed is reached, it is necessary to achieve a positive lift (with the vehicle in lift-up attitude) then the vehicle decelerates in order to realize a flight at constant altitude until the suborbital branch of the equilibrium upper boundary is encountered. At this point, the angle of attack is kept fixed at its maximum value, in order to follow the upper boundary of the entry corridor. In this case the bank angle is used only to obtain full lift up to an AoB=0 and full lift down to an AoB=180. The angle of attack is modulated between 45° and about 5°. When the orbital speed is achieved the stagnation point heat flux is strongly reduced and therefore the aerothermal environment is not more a critical issue. The suborbital branch of the trajectory then can continue with fixed angle of attack.

The same trajectory, in the altitude-velocity plane, can be performed in a completely different way if the same lift modulation is accomplished with constant angle of attack but modulating the bank angle.

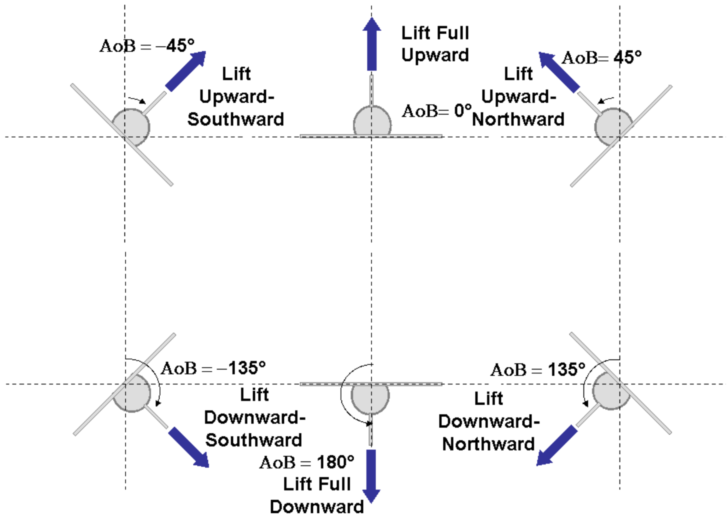

Figure 2-12: Roll angles denominations

The objective is to generate the same lift at the same altitudes but with a fixed angle of attack, using roll modulation. Figure 2-12 introduces the roll angle nomenclature. While the angle of attack is held constant at 45°, the bank angle is progressively reduced from 180° to 0 so that the vehicle flight is controlled at constant altitude. The trajectory is the same in the velocity-altitude plane but the duration is much less in comparison to the pitch-modulation case.

In case no cross range is required then the roll angles will assume negative and positive values and with zero time average. If cross ranges are necessary then the duration of the positive and negative roll angle will not be the same.

In any case this trajectory is more critical for the heat fluxes to the exposed belly side surfaces because the angle of attack is constantly larger than pitch control modulation.

Two different modes have been investigated in order to follow the same flight path in the velocity-altitude plane but with a mixed control, i.e. modulating pitch and roll.

In the first mode the bank angle is initially held constant while pitch modulation is accomplished modulating the angle of attack from the initial value of 45° until it reaches a value of 20°. After this point the angle of attack is held constant and lift modulation is continued by roll changing the bank angle from 180° to 0°. At this point zero bank angle is maintained and the angle of attack is increased up to 45° to keep the vehicle along the prescribed trajectory.

In the second mode, lift is modulated essentially by pitch modulation changing the angle of attack similarly to the first case. The main difference is that the bank angle is initially 180° and the vehicle attitude is reversed from lift down to lift up when the orbital velocity is reached. When the orbital speed is reached the vehicle attitude is reversed changing the bank angle to 135°. At the maximum latitude the bank angle is changed from 135° to 45° in order to further increase the cross range. Finally, when the maximum angle of attack is reached lift is modulated by roll reducing the bank angle from 45° to zero.

The main differences are evident in the ranges. The trajectory obtained with pitch modulation only corresponds to the maximum down-range (about 40000Km) and zero cross range. The trajectory corresponding to roll modulation provides a relatively small down range (about 10000 Km) and a cross range of about 750 Km.

In the first mixed control mode the down range is about 32000 Km and the cross range is less than 200 km because the trajectory is not optimized to increase the cross range. In the second mode the down range is about 34000 Km (i.e. comparable to the maximum possible obtained with pitch modulation) and the cross range is the maximum (about 1500 Km).

The cross range can be larger if the vehicle flies for a larger part of the trajectory at relatively lower angle of attack (e.g. AoA<20°). This can be accomplished after that the vehicle has been decelerated at orbital speed, as discussed in the section dedicated to innovative re-entry trajectories from LEO. Instead, in order to avoid exposing the belly side to the high heat fluxes, the suborbital phase of the trajectory can be performed.

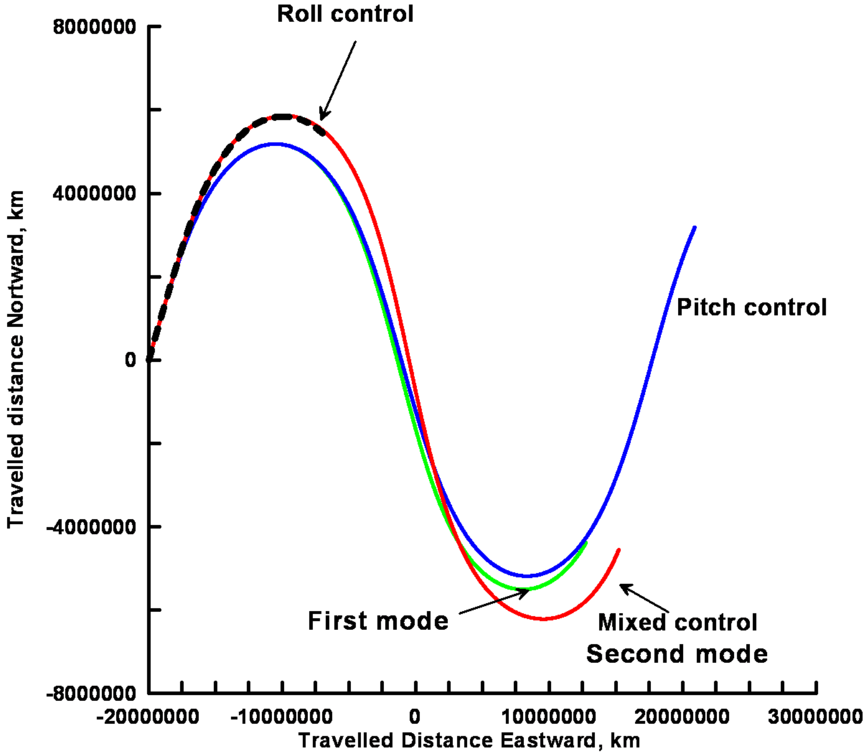

Figure 2-13: Range. Comparison between different modes of lift modulation

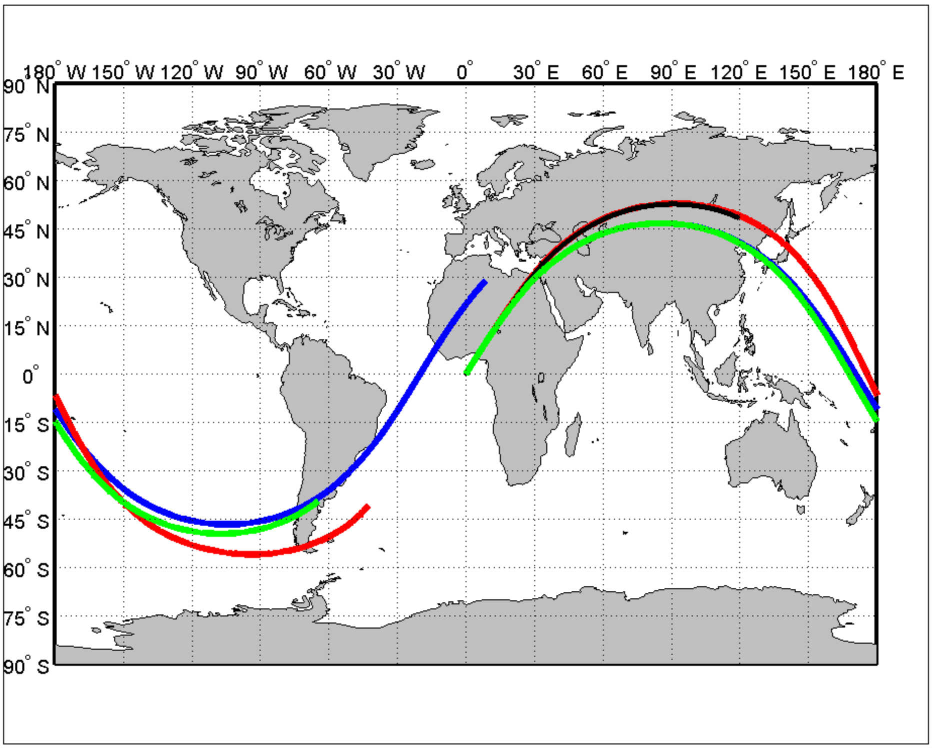

Figure 2-14: Ground tracks. Comparison between different modes of lift modulation. Blue line: Pitch control; Red line: Mixed control, second mode; Dashed line: Roll control

Even though there is the possibility to modulate both AoA and AoB to change the lift force it is more convenient to modulate AoA and leave AoB for achieving the desired cross ranges instead of using AoB modulation because this will imply larger AoA and a higher heat flux over the structure.

Concluding it may be said that these gliding trajectories show the flexibility of the proposed innovative vehicle, in principle, to manoeuvre in both pitch and roll modes. Anyway, the choice of the best control law is mainly dictated by thermal and range considerations that will be assessed only when reference vehicle configuration and reference mission will be identified. Further this choice depends also strongly on the technical solutions for the different subsystems (i.e. for aerothermal problems the availability of hot structure materials, TPS, insulating materials for crew aeroheating protection, etc.).

As in the case of LEO return, possible re-entry trajectories from exploration missions have been computed with the same initial conditions at the entry interface as it was already analyzed in the previous paragraph. In this case, in order to limit the re-entry duration and the crew cabin overheating a “constant heat flux” trajectory is considered, corresponding to the first leg of the lower boundary trajectory inFigure 2-7 red curve. This trajectory has been implemented by proper aerodynamic force modulation using pitch control, for different bank angles.It is interesting to see that increasing the bank angle the trajectory duration and therefore the range is reduced. In particular the down range is reduced from 13000 Km to 11000 Km and the maximum cross range, corresponding to a bank angle of 45° is about 1000 Km.

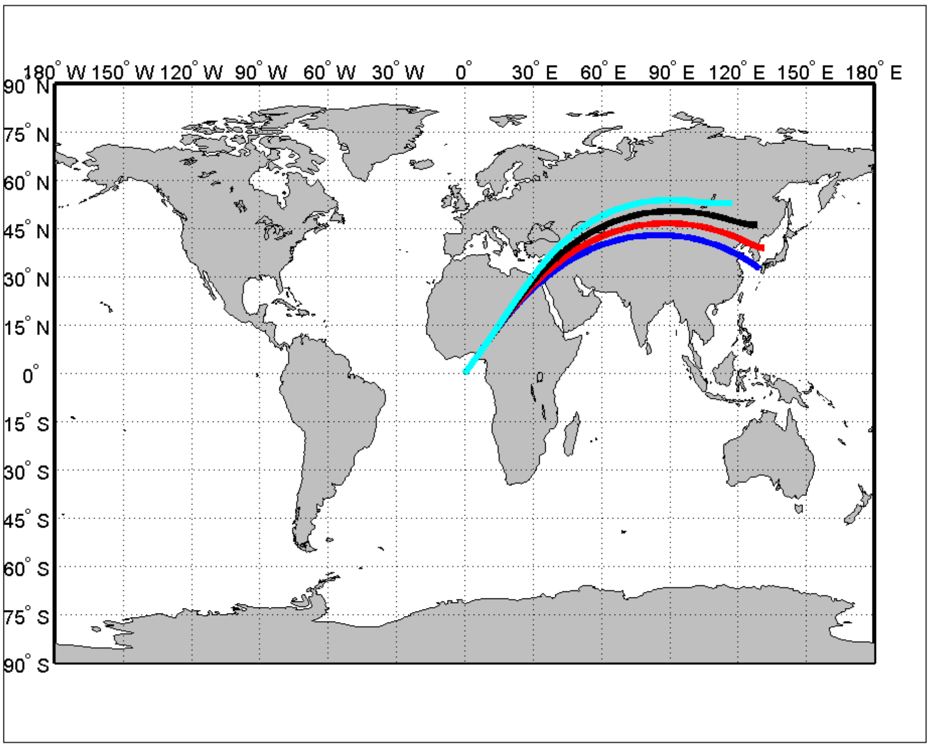

Figure 2-15: Ground tracks. Pitch control along the lower boundary boundary with different bank angles

The most important parameters evaluated along the computed trajectories for re-entry from Moon will be referred to the trajectories along the upper boundary of the entry corridor in the altitude-velocity plane, blue curve in Figure 2-16 and to the trajectories corresponding to the lower boundary, red curve in Figure 2-16. The former can be obtained modulating the lift force using pitch, roll, or mixed control. The latter is obtained modulating lift and drag by pitch control only. The different trajectories have been summarized in Figure 2-17 showing the altitude versus time.

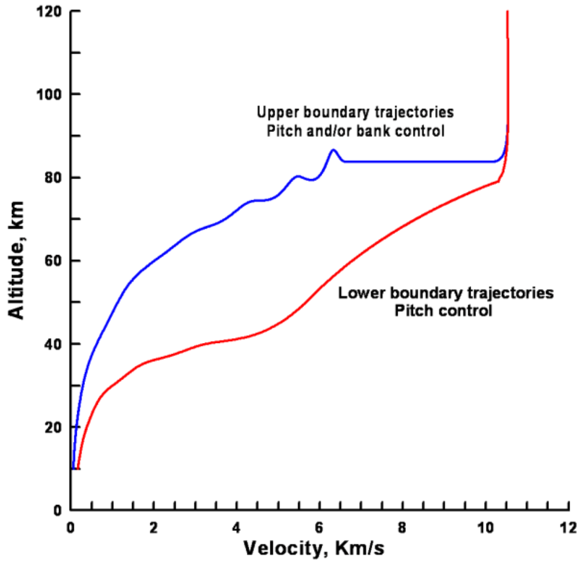

Figure 2-16: Altitude versus velocity. Summary of different re-entry trajectories

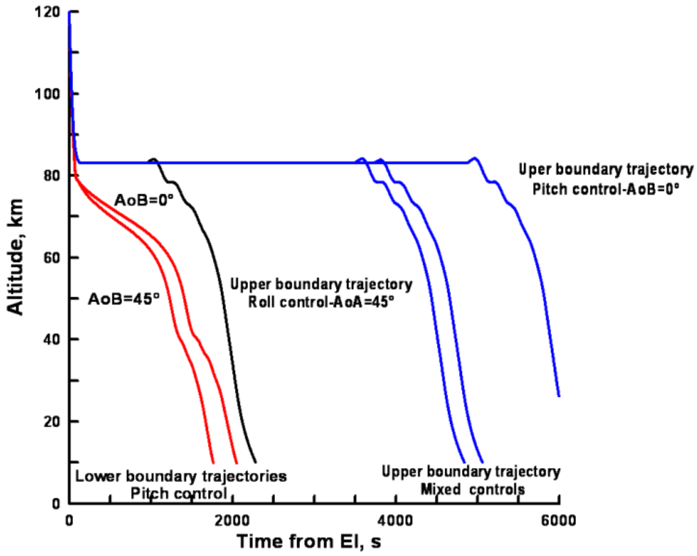

Figure 2-17: Altitude versus time. Summary of different re-entry trajectories

The upper boundary trajectory performed using pitch control only and zero bank angle has the longest duration (about 6000 s). The upper boundary trajectories using mixed control, i.e. both angle of attack of attack and bank modulation, have intermediate duration (in the order of 5000s). The upper boundary trajectory based on roll control only, maintaining a constant angle of attack of 45° has a duration of the same order of magnitude of the lower boundary trajectories (about 2000 s). The corresponding diagrams of the altitude, velocity, heat flux, temperature, deceleration versus time are shown in Figure 2-18 to Figure 2-21. It is interesting to note that the stagnation point heat flux is almost constant along the lower boundary trajectories (red lines); on the contrary, the upper boundary trajectories exhibit a peak in the heat flux in correspondence of the aerocapture into the atmosphere followed by a decreasing trend while the vehicle decelerates at almost constant altitude

Figure 2-21 shows the total deceleration versus time for the different trajectories. The maximum deceleration is about 1.2g for the upper boundary trajectories, while the lower boundary trajectories exhibit a relatively large deceleration with a peak of 2g due to the lower altitude reached at the highest velocities.

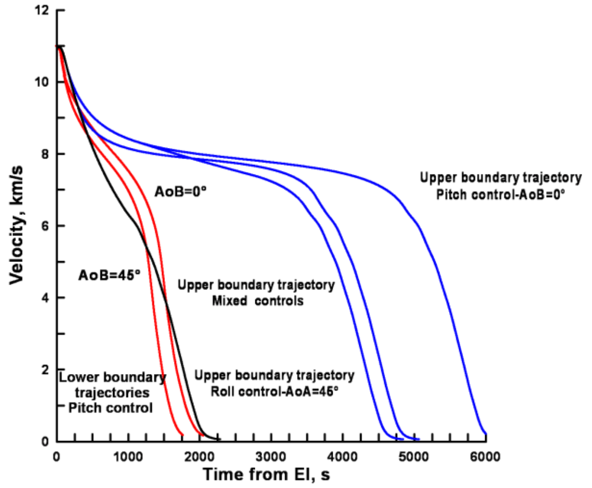

Figure 2-18: Velocity versus time. Summary of different re-entry trajectories

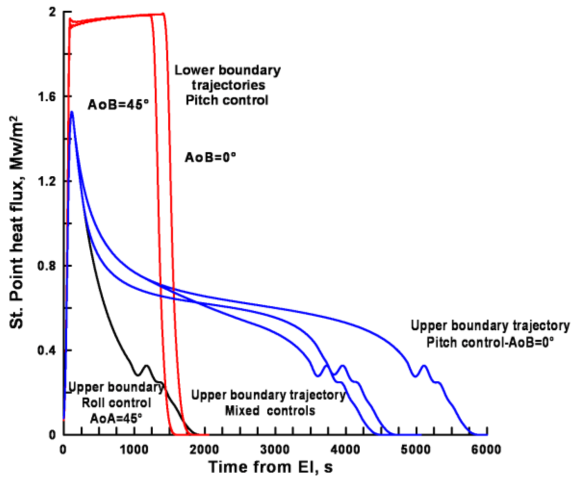

Figure 2-19: Heat flux versus time. Summary of different re-entry trajectories

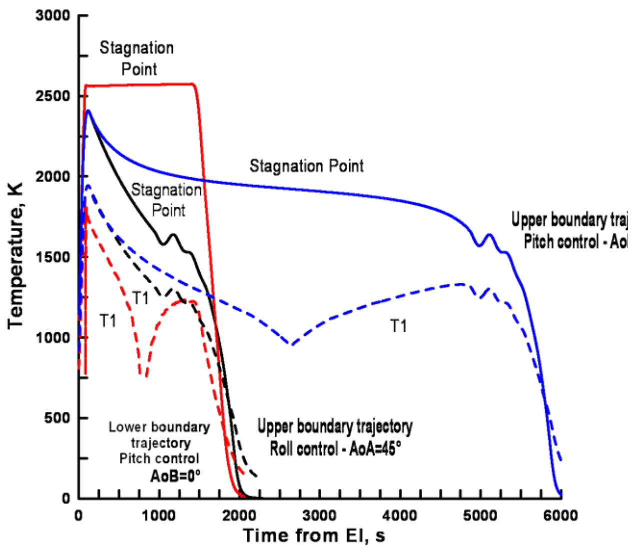

Figure 2-20: Radiation equilibrium temperatures. Summary of different re-entry trajectories

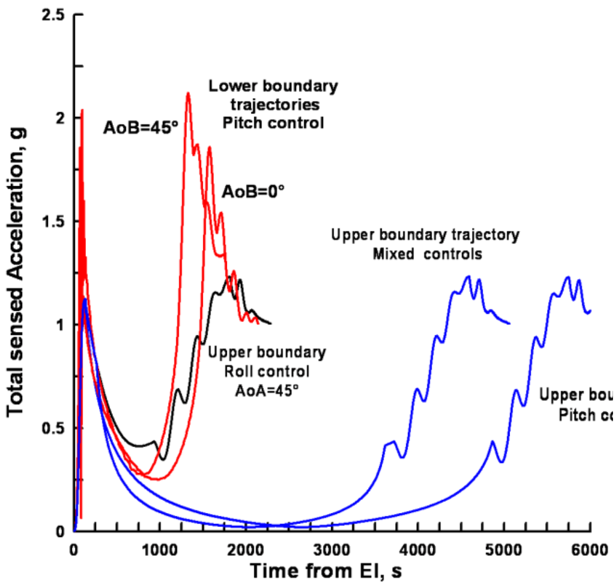

Figure 2-21: Deceleration versus time. Summary of different re-entry trajectories

One other solution is to accomplish a mixed re-entry strategy (constant altitude at the super-orbital velocities and constant heat flux at suborbital velocities. The results of this assumption have been illustrated in Figure 2-22 to Figure 2-27.

It is interesting to see that with the mixed strategy (a constant altitude leg until the velocity reaches about 7km/s and an angle of attack of about 20°, followed by a constant stagnation point heat flux leg at value in the order of 0.5 MW/m^2) the time history of the total deceleration is not very different in comparison to the upper trajectory, the stagnation heat flux is held constant when a relatively low value is obtained and the re-entry duration increases because the angle of attack is lower during the final leg of the trajectory, and this implies higher L/D.

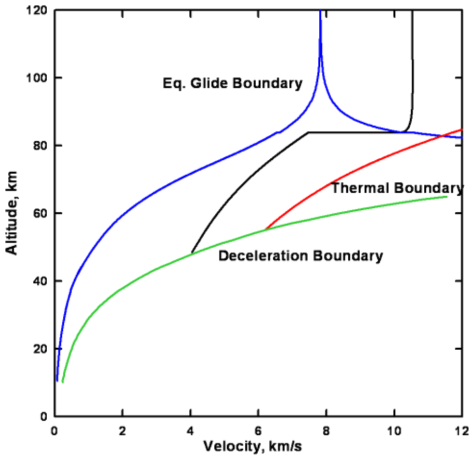

Figure 2-22: Altitude versus Velocity. Trajectory with mixed strategy and corridor boundaries.

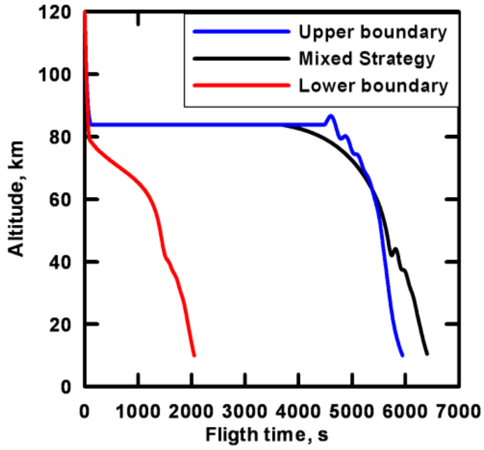

Figure 2-23: Altitude versus time. Mixed strategy and upper and lower boundary trajectories

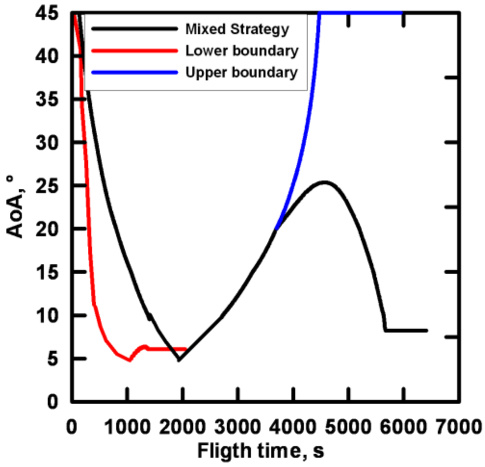

Figure 2-24: AoA versus time. Mixed strategy and upper and lower boundary trajectories

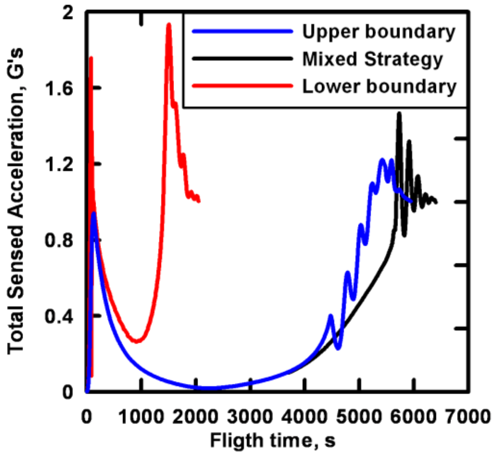

Figure 2-25: Deceleration versus time. Mixed strategy and upper and lower boundary trajectories

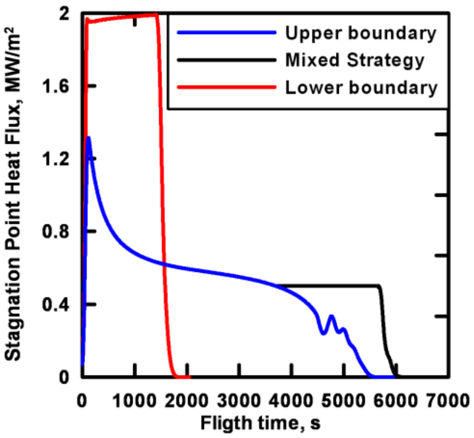

Figure 2-26: Stagnation point heat fluxes versus time. Mixed strategy and upper and lower boundary trajectories

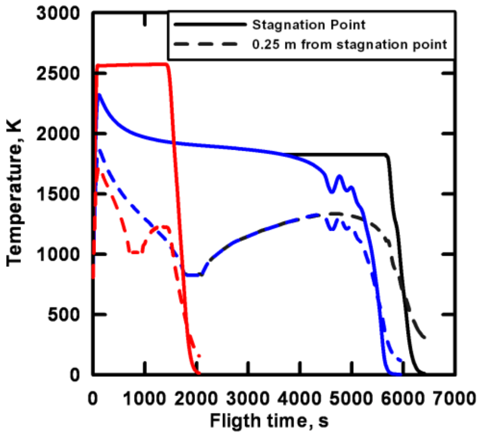

Figure 2-27: Radiative Equilibrium Temperature versus time. Mixed strategy and upper and lower boundary trajectories

3 TYPICAL MISSIONS & PARAMETERS FOR EARTH ENTRY

The definition of typical High Lift Re-entry Vehicle missions along with the corresponding relevant entry parameters concentrates on the following three different scenarios:

- Return from LEO (e.g. ISS mission)
- Return from Moon
- Return from Mars

Hereby, the main entry parameters comprise:

- Atmospheric entry altitude
- Atmospheric entry angle (flight path angle at entry interface)
- Atmospheric entry velocity
- Latitude, longitude and heading angle at the atmospheric entry point
- Time of entry as date and/or local time (day/night)

By nature, atmospheric entry altitude is not a free parameter, but usually set to a fixed value. In this study the entry at 120 km altitude has been assumed. Also, the entry angle cannot be seen as free parameter, although from the mission analysis point of view, a very high range is achievable for each mission. Instead, there are limitations resulting from the system design and it is usually useless to discuss high ranges for this critical parameter. In the following analysis, the entry angle was set to -5°, which is seen as a representative value for High Lift Re-entry Vehicles.

3.1 LOW EARTH ORBIT (LEO)

If considered from the exoatmospheric mission analysis point of view, return from a low Earth orbit is the simplest of the three scenarios. There is no large range of typical entry velocities, which only depend on the LEO orbit inclination, as result of the rotational motion of the atmosphere, contributing to magnitude of the entry velocity. Also limited by the orbit inclination of the LEO orbit, the range of reachable latitudes at entry point is given. For instance, the entry point can be freely selected between 51,6° S and 51,6° N (see Figure 3-1) if the LEO inclination is 51,6° (ISS-Orbit).

In a nominal mission scenario, a nominal atmospheric entry point will be defined a priori and will be reached by an appropriate selection of the de-orbit burn time and location. In a contingency scenario, this flexibility is possibly not given. Instead, one has to cope with the entry point location and entry time according to the time and location at the occurrence of the contingency event. Only if some delay is acceptable by the contingency event, one can influence the entry point location by staying in orbit for some few orbital revolutions. If not time is left, the de-orbit must be performed immediately and the current location of the entry point must be accepted. Therefore, in a worst case scenario all entry points as indicated in Figure 3-1 (yellow latitude range) can possibly be reached.

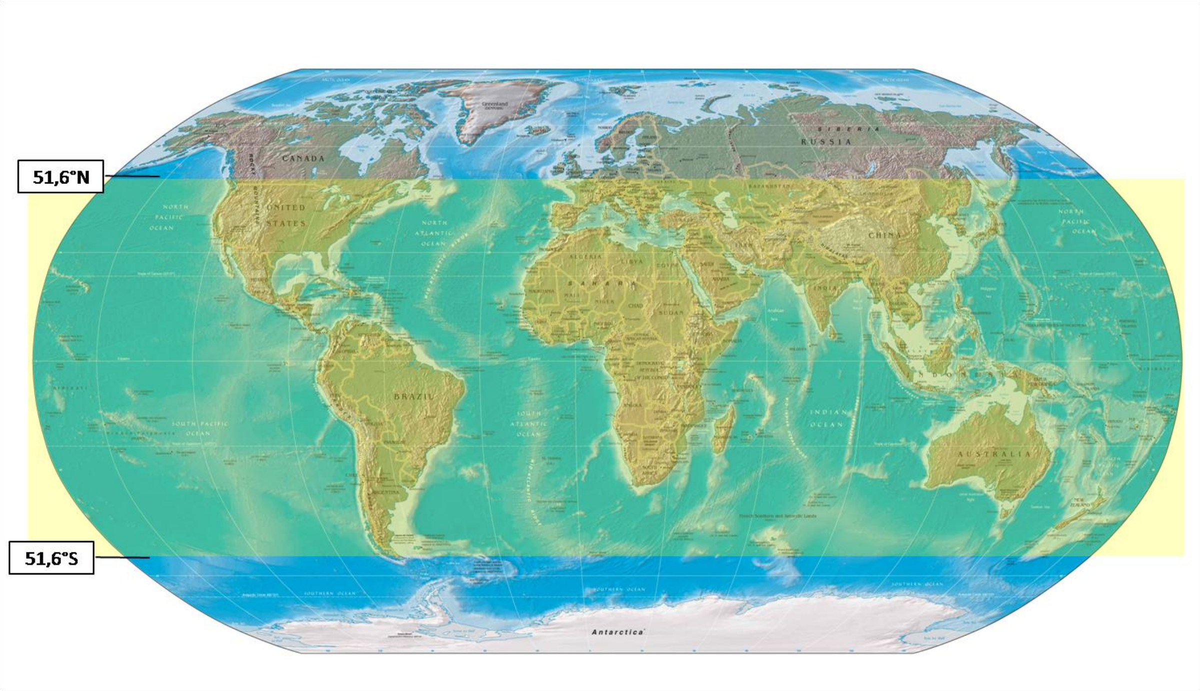

Figure 3-1: Entry Corridor for a 51,6° Inclination LEO-orbit (ISS)

3.2 MOON

Of the three Earth return options listed at the beginning of this section, return from the Moon is the most complex one when considering the number of options to be accounted for. On the one hand, this scenario is not as limited as for Mars missions. On the other hand, the flexibility is more limited than for LEO missions so that a higher number of constraints must be considered in the corresponding analysis.

In general, return from the Moon is possible every day at minimum ΔV cost, if sufficient flexibility with respect to the entry latitude is given. On the other hand, if constraints on this parameter are imposed, the number of return opportunities reduces quickly.

There are some important characteristics of lunar transfers which must be taken into account for the analysis of this scenario:

- The inclination of Moon's orbit around Earth varies between 18.3° and 28.5°, as consequence of the regression of its ascending node in the heliocentric frame (on the ecliptic plane). The full cycle takes 18.6 years.

- Depending on Moon's orbit inclination at a given epoch, the inclination of the return trajectory orbit (with respect to equatorial plane) must be allowed to reach the inclination of the Moon's orbit around Earth if return at any time is required.

- Return from the Moon will be always such that braking in the geocentric frame is performed at Moon (Moon escape maneuver) to reach the return trajectory by lowering the orbit perigee.

- During the escape burn from the Moon (or slightly after), a small maneuver can in principle be performed to (slightly) change the orbit plane and therefore get some flexibility with respect to entry point selection. However, the range of reachable entry points is limited if propellant mass of the returning vehicle must be minimized and this is a valid assumption for a High-Lift Re-entry Vehicle.

In fact, the last point shows one of the main advantages of the High Lift Vehicle concept. Since a long atmospheric flight is performed (large downrange and crossrange by nature) the entry point can be located far from the landing site. In this way, the entry point can be selected such that propellant needed to reach it from the exoatmospheric flight is limited, widely independent from the landing site.

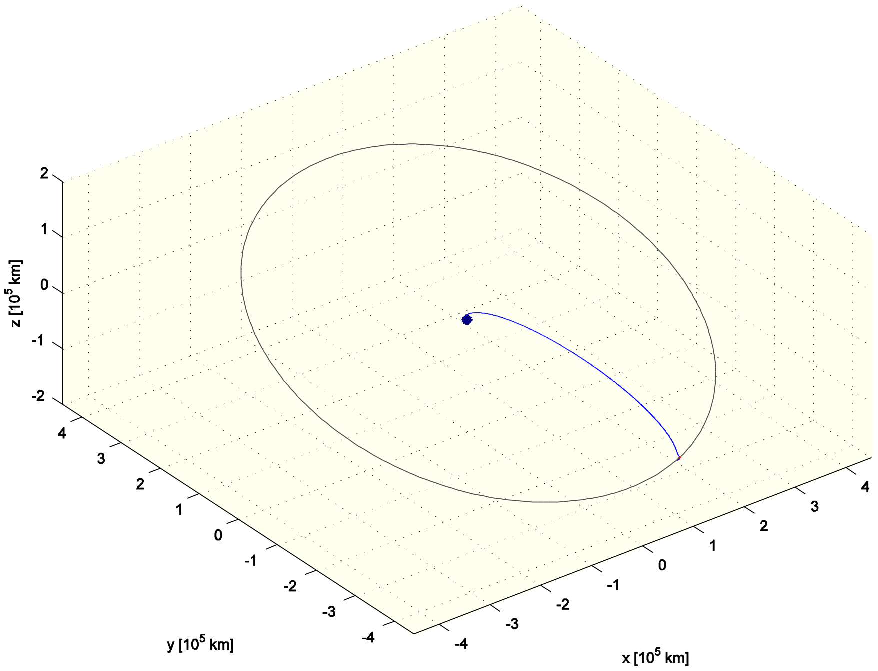

Figure 3-2: Moon return trajectory in September 2018 (as representative case)

For a particular epoch (end of 2018) the Moon return scenario has been investigated in more detail. Figure 3-2 shows a representative Moon return trajectory in the geocentric frame. The xy-plane corresponds to the equator plane, x-direction pointing towards the vernal equinox. Moon's orbit around the Earth is plotted as dark line. Its inclination of about 22° can be seen from the figure.

The return mission begins with the Moon escape maneuver, which is assumed to be performed in a polar circular orbit of 100 km altitude. The periselenium of the escape hyperbola is optimized such that optimum return trajectory is reached. The escape direction is always opposite to Moon's velocity vector on its travel around Earth, to reduce the geocentric velocity. This is shown in Figure 3-3, where the maneuver is shown in red color. (Also in this plot the xy-plane is the ecliptic plane, although the coordinate system is selenocentric.)

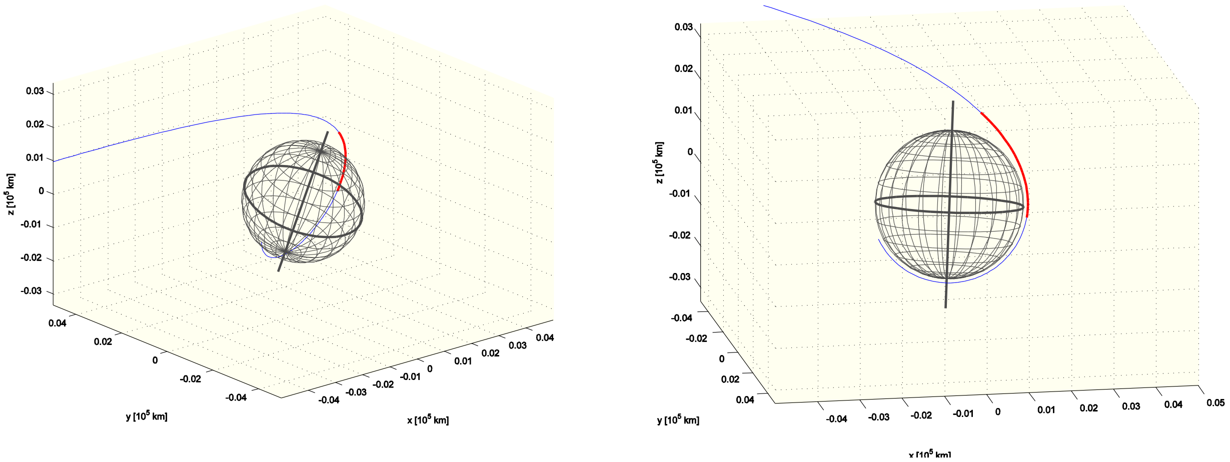

Figure 3-3: Moon escape from 100 km polar orbit (maneuver plotted in red color)

After a travel of about 5 days, the atmospheric entry is performed. The approach trajectory is presented in Figure 3-4 for the particular case, that the latitude of the entry point is 27.5° N. The inclination of the return trajectory is optimized to be around 49° for this case. At entry, the vehicle is flying towards South on such inclined orbit. Assuming an atmospheric flight taking around 3/4 of a full Earth orbit (i.e. about 270° of true anomaly) the vehicle can reach a European landing site in this way. This is exactly the advantage of the High Lift concept as discussed above. A large downrange allows for a significant distance between the entry point and the landing site, in contrast to more conventional systems.

Note that Figure 3-4 shows two views of the same trajectory to allow the reader to better understand the scenario.

Table 3-1 summarizes some main characteristics of the presented scenario. An initial mass of 10000 kg in lunar orbit has been exemplary assumed. Assuming a thrust level of 5000 N (and therefore an initial thrust to mass ratio of 0.5 N/kg) a ΔV of 859 m/s is required to escape the Moon and lower the perigee of the return trajectory to lead to atmospheric entry.

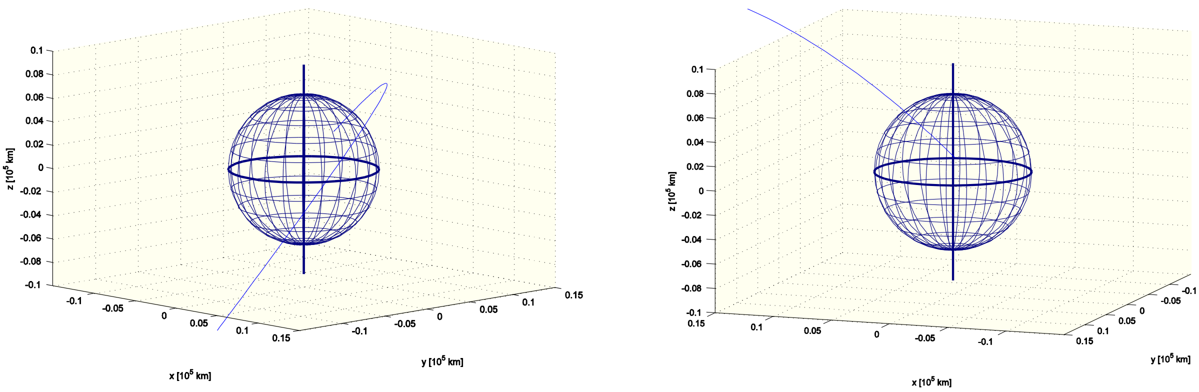

Figure 3-4: Earth approach for atmospheric entry at 27.5° N

The entry angle was set to -5° as a typical value for the High Lift Vehicle. This was achieved by setting the perigee altitude of the elliptic return orbit to about 70 km. The entry velocity at entry point results to 10.68 km/s. The orbit inclination is close to 49°, the orbit is therefore prograde and the rotational motion of the atmosphere is used to reduce the entry velocity, which would be slightly in excess of 11 km/s otherwise.

Moon Return Characteristics (Example)	
Departure at Moon	19 Sep 2018
Initial mass	10000.0 kg
Propellant mass for escape	2394.4 kg
ΔV for escape manoeuvre	859.2 m/s
Arrival at Earth	24 Sep 2018
Entry mass	7605.6 kg
Entry angle	**-5.0 °**
Entry velocity at 120 km	**10.679 km/s**
Entry latitude	**27.5 ° N**
Earth orbit inclination	48.8 °
Entry local time	6.835 Hours

Table 3-1: Main characteristics of the Moon return transfer example

In this scenario, entry is performing in daylight, shortly after sunrise. If atmospheric entry during night shall be avoided, this parameter becomes the next one to be included in the scenario definition and optimization process. The impact would be with respect to the limitation of the return opportunities during one lunar month, or on the need to consider retrograde entry as a possible option, significantly increasing the atmospheric entry velocity.

In the second step of the analysis of the Moon return scenario, the impact of the entry latitude on the overall scenario has been analyzed. This was done by means of a parameter analysis during which the scenario was re-optimized for any entry latitude selected.

The results are presented in Figure 3-5 and Figure 3-6. The plots in Figure 3-5 show the evolution of the orbit inclination, the entry velocity and the local time at entry as function of the entry latitude. The entry latitude varies between 0° and 42° N in this analysis and the entry is from a prograde orbit.

Figure 3-6 presents the evolution of the Moon escape ΔV along with the entry mass which is the initial mass of 10000 kg reduced by the propellant mass needed for Moon escape. In the lowest plot the time of atmospheric entry in MJD2000 days is given (MJD2000 = 6841 corresponding to 24 Sep 2018).

From the figures one can see that both, the entry velocity and the required propellant mass for Moon escape practically remain unchanged for an entry latitude range of 0° - 22°, while both parameters drastically increase for higher latitudes. This can be explained by considering that the inclination of the Moon's orbit around Earth is close to 22° at this epoch. (Thus, depending on the epoch, the same behavior will occur up to entry latitudes of about 28°).

For the reference case of September 2018, the return ellipse can be optimized such that its apogee is close to the Moon after escape as long as the entry latitude stays below 22°. In particular, if 22° N are required, one can select the optimum departure point on the Moon orbit around Earth close to a true anomaly of 270°, i.e. just between the descending and ascending node (as shown in Figure 3-2). Then, the apogee is at 22° S and the perigee (and therefore also entry latitude) is close to 22° N. If, in contrast, the entry latitude of 0° is required, the optimum departure point moves to one on the nodes, since at this point the apogee of the return ellipse can be selected to by around 0° without ΔV penalties.

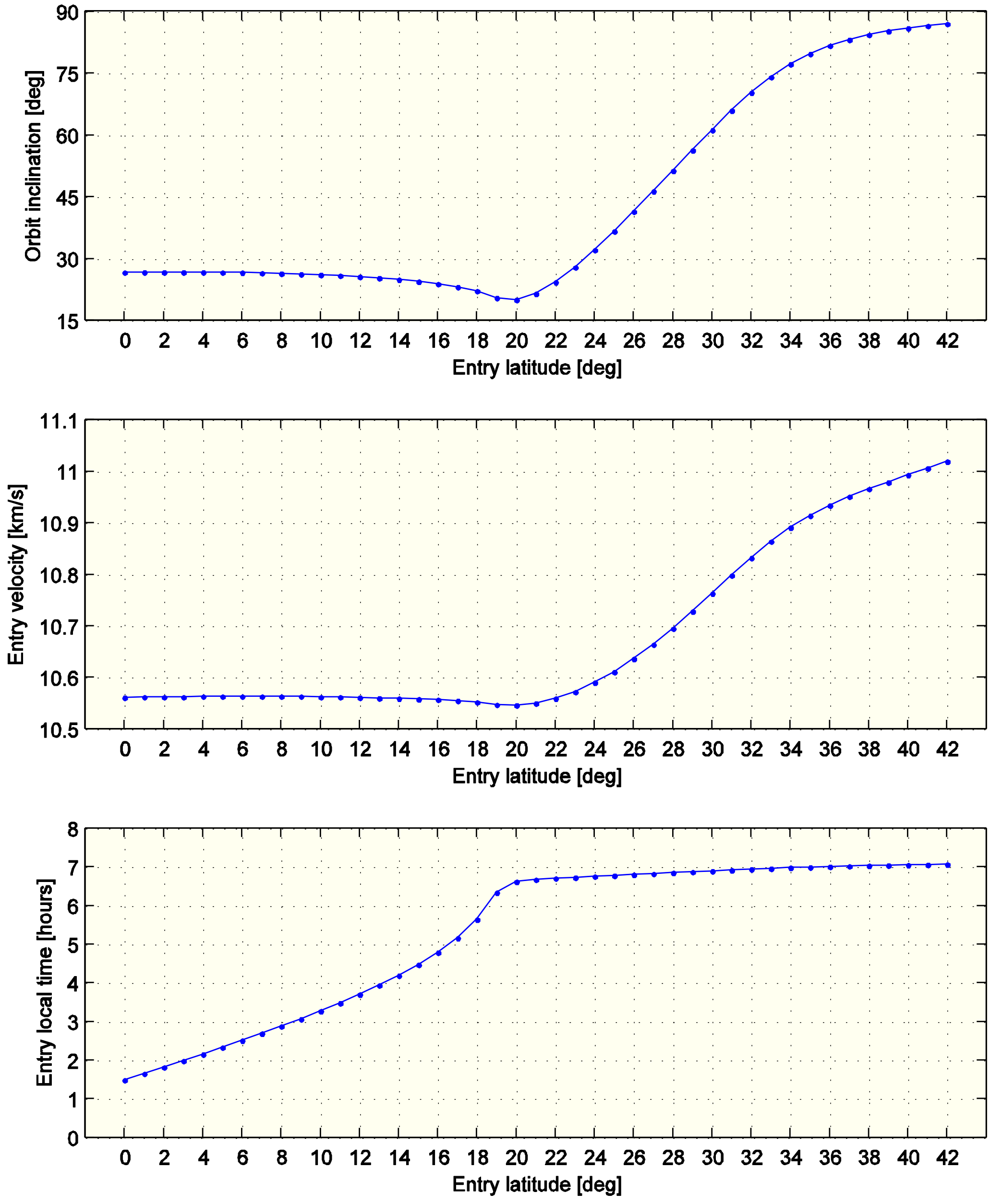

Figure 3-5: Parameter analysis with respect to entry latitude (1)

This variation of the escape/entry time can be seen from the lowest plot in Figure 3-6, where the distance in time between 0° and 22° is around 7 days, which is a true anomaly distance of about 90°.

If, in contrast, the entry latitude is required to be higher than 22° N, the apogee of the return ellipse must also reach such a high value on the Southern hemisphere. This cannot be done by selecting the optimum position of the Moon on its orbit, due to the limitation of 22°. Instead, the escape maneuver must inject the spacecraft on the ellipse with such a Southern apogee, which can be only done by injecting on the position away from the apogee (true anomaly higher than 180°). By nature, this injection strategy is more costly from the ΔV point of view, which is reflected in the plots.

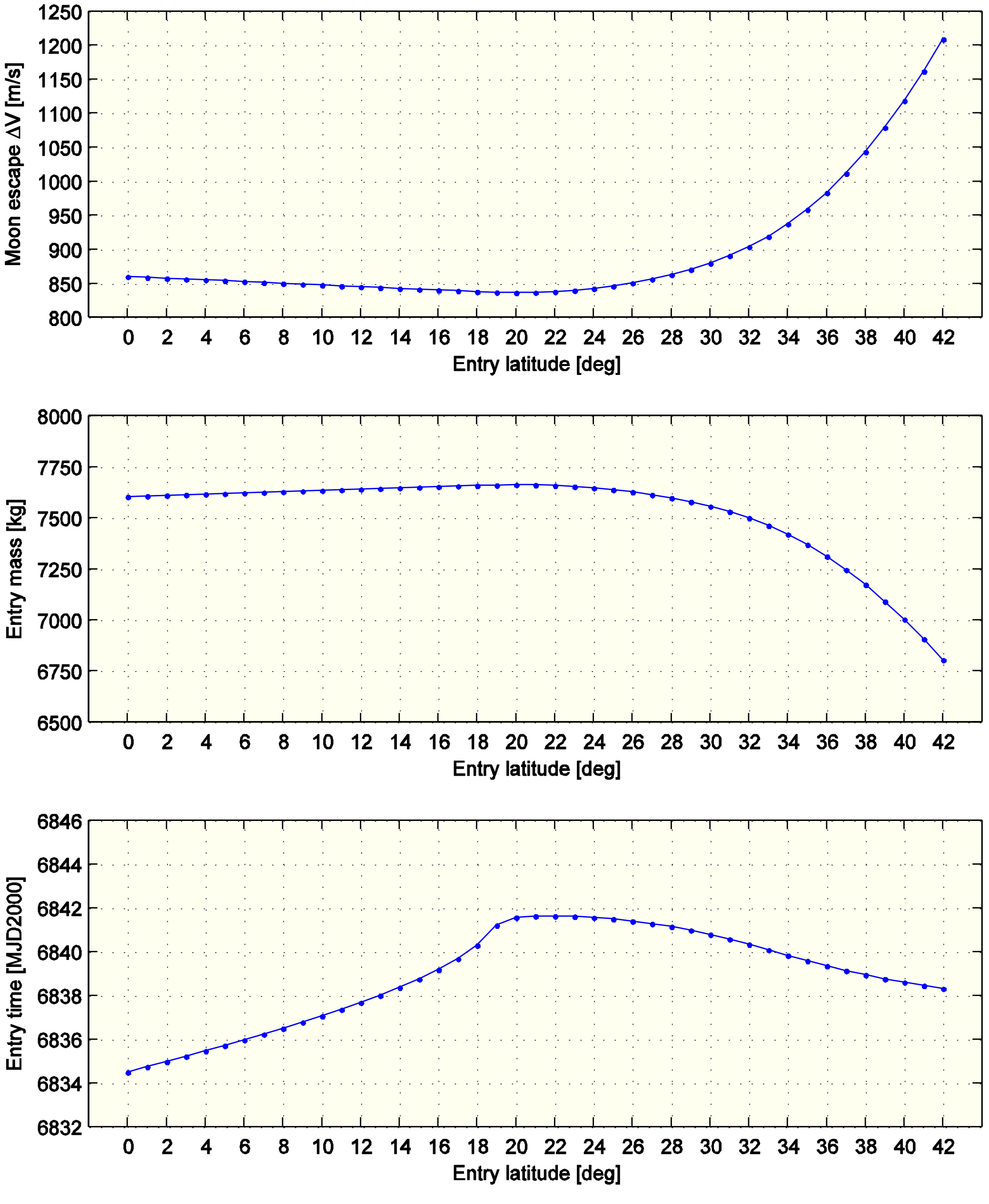

Figure 3-6: Parameter analysis with respect to entry latitude (2)

From the figures one can also see, that entry latitude of 42° is already close to the limit. The return ellipse has an inclination of almost 90° in this case, so that the spacecraft is flying over the North Pole before entry. Higher entry latitudes are not possible within a reasonable ΔV budget, since the resulting ellipses would not cross the Moon's orbit around Earth anymore. A sequence of maneuvers would be required, resulting in unacceptable propellant masses needed.

As result of this analysis, one can conclude, that the nominal entry latitude range for return mission from the Moon shall not exceed the range of about 28° S – 28° N. In this way, the propellant need for Moon escape stays almost constant and return to Earth at any time is possible. This is illustrated in Figure 3-7.

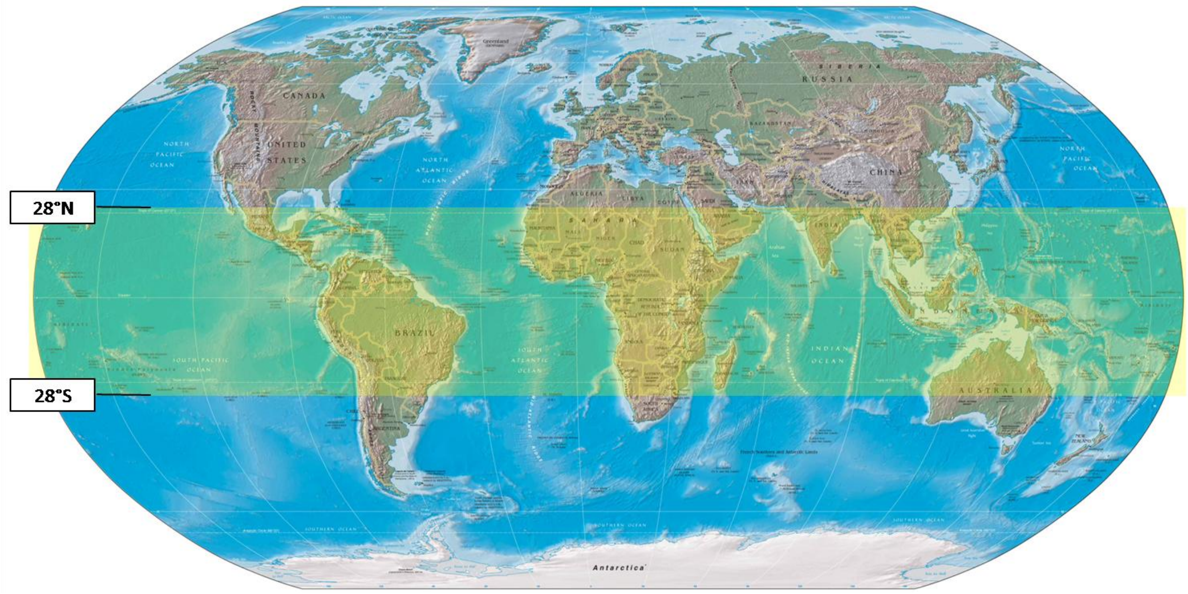

Figure 3-7: Entry Latitude Range for Moon Return

If the High-Lift Re-entry Vehicle can cope with this full range of entry points (latitude between 28° S and 28°N and all longitudes) than one can cover both nominal and contingency cases without problems. If the concept can support the above range only partially, then particular attention must be paid to contingency cases.

This is due to the fact that the contingency cases are mainly characterized by a non-nominal entry point location (latitude and longitude). The nominal case of return from the Moon already covers the worst case entry velocity, as it is highest in this case. In that sense, contingency cases for Moon missions can be defined as follows:

- Contingency event during the Earth-Moon transfer – depending on the geocentric distance at contingency occurrence, the mission can be interrupted by performing a maneuver leading to the immediate return to Earth, without reaching the Moon. In this case, the entry velocity is lower than in the nominal case as the apogee altitude is below the Moon distance.

- Contingency event during proximity operations at Moon – in this case the entry velocity is same as for the nominal case as apogee altitude of the return orbit is the same.

A contingency event can therefore only have the consequence of a non-nominal entry point location within the latitude range shown in Figure 3-7. This is due to the entry time which can (probably) not be freely selected in case of contingency. Thus, if the above range of entry latitudes / longitudes cannot be supported by the vehicle concept, not allowable latitude / longitude combinations must be defined and excluded from the set of acceptable entry points for the return trajectory. This will translate in time one will have to wait in Moon orbit (or before performing a turn maneuver during the Earth-Moon transfer) such that the entry point will be covered by the set of entry locations supported by the vehicle.

In contrast, one can freely select the time of return to Earth in a nominal scenario. Thus, one can always define a return mission such that the entry will take in the particular area of the range shown in Figure 3-7. The maximum time to pay will be a full Moon revolution around Earth (so about 28 days) but only if a single entry location area is allowed. This is, however, not expected for the High-Lift Re-entry Vehicle, so more flexibility will be granted.

3.3 MARS

Note: In agreement with ESA a mission from Mars will not be handled in detail in this study due to the limited utilizability of the reference vehicle. So the Mars missions will be described only in the related technical notes of this study.

4 LAUNCH AND LANDING SITES FOR A HIGH L/D VEHICLE

4.1 PREFERRED LAUNCH SITES

For the selection of suitable launch and landing sites all over the world for the PHOEBUS HL-3A vehicle the following main requirements are considered:

- Preferred in European territory
- Ascent phase over water or unoccupied respectively low populated area
- Facilities for maintenance, integration and manufacturing due to reusability aspects are available nearby
- If in situ manufacturing is not foreseen or possible, transport connection to harbour for shipping or big runways and infrastructure for large airplanes like Airbus 380 or Beluga shall be available.
- The reference scenarios for this study are a mission to the ISS (LEO, inclination of 51,6°) and a Moon mission (inclination of max. 28°).

Furthermore the launch characteristics of the different Launch sites have to be considered, which are:

- Launch sites that launch in the East direction launch with the rotation of the Earth, hence they provide already a certain amount of delta v.
- Launch sites that launch in the direction of water will have a smaller risk with respect to populated areas then launch sites that have to launch over land.
- Different launch sites will launch with different inclinations which will impose the necessity of different “plane change” corrections.

This leads to a variety of best suitable land launch sites, listed in Figure 4-1.

Figure 4-1: Suitable Launch Sites

For the reference scenarios for this study to LEO and Moon the launch directions from Kourou considers the most safety aspects wrt staging. This means the first (or second) Stage of a rocket shall descent in unmanned areas - favored on water. This leads to the following launch directions (see also Figure 4-2):

- ~ 5° S for e.g. Moon missions
- ~ 50° N for e.g. ISS missions
- ~ 80° N for polar missions

This also allows more flexibility for abort cases.

Figure 4-2: Typical launch Directions from Kourou

The alternative launch solution of a sea launch is quite out of the question due to the limit of the launcher payload of max. 6100 kg into LEO. This is not sufficient for the transportation of the complete PHOEBUS vehicle (including resource module).

4.2 PREFERRED LANDING SITES

The selection of the possible landing sites for the SpacePlane demands a detailed examination of the requirements for this vehicle.

Among the technical requirements also political aspects shall be considered. The mission specific requirements can differ as well as the requirements for abort and contingency cases.

The PHOEBUS landing sites are based on the nominal and abort landing sites of the Space Shuttle due to comparable specifications. In principal all military and civil airports with runways and a suitable infrastructure can be used.

The nominal landing sites shall be selected considering the following issues:

- Location preferred on European territory
- Facilities for maintenance, integration and manufacturing due to reusability aspects shall be available nearby
- Preferred close to launch site
- Descent phase during approach and landing over water or unoccupied respectively low populated area
- Descent area shall be large, plain areas without obstacles like hills or large buildings etc.
- If landing nearby launch sites is not possible, transport connection to harbour for shipping or big runways and infrastructure for large airplanes like Airbus 380 or Beluga shall be available
- For transport of the SpacePlane after landing the runway shall have an adequate carrying capacity (for A380, A300-600ST [Beluga], ...)
- Runway shall have a minimum length of 3000m and 40m width
- Due to automatic landing navigational aids assisting safe landing shall be available
- Low frequented airport
- For the nominal and for abort/emergency cases, locations with all of the necessary equipment to handle a normal landing as well as Abort Once Around (AOA), Abort to Orbit (ATO), Transoceanic Abort Landing (TAL) and Return to Landing Site (RTLS) abort can be used1.

The nominal landing sites shall combine the requirements for the SpacePlane vehicle and the infrastructure to the best solution wrt economic and political aspects.

As an important technical design driver the down- and crossrange is obvious important. As an example (here for an entry latitude of about 20°) Figure 4-3 shows the maximum downrange of about 36.000 km and a maximum crossrange of about 3.500 km. This enables to reach a wide range of landing sites

[1] http://space.balettie.com/LandingSiteInfo/index.html

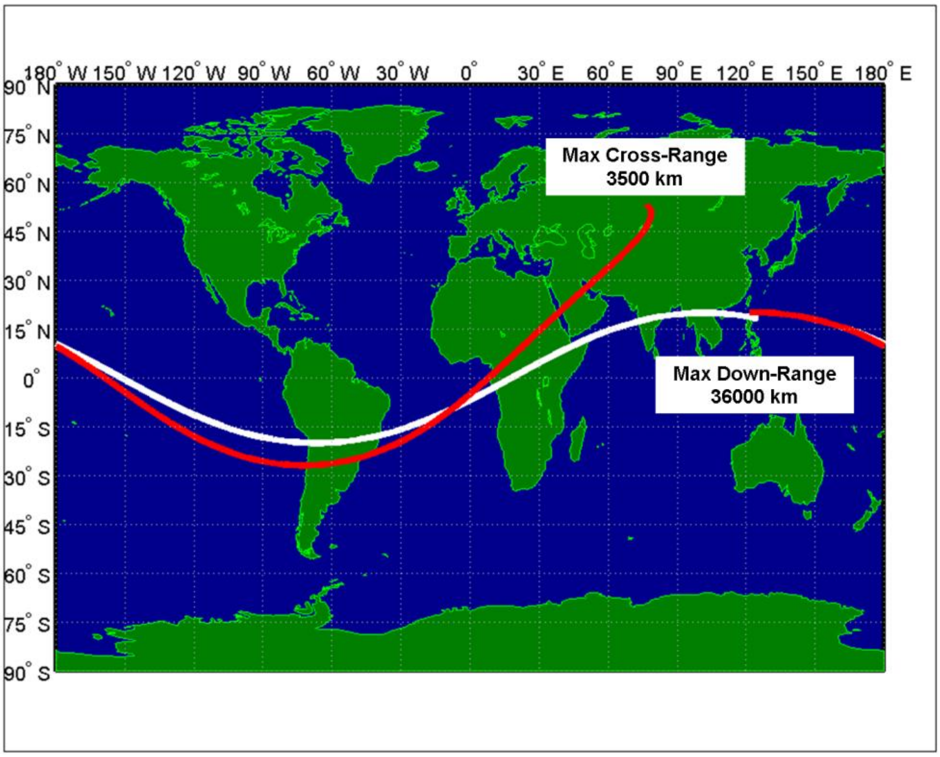

Figure 4-3: Maximum down-and crossrange

After analysis of the landing sites characteristics wrt the requirements described before three preferred landing sites for nominal cases are shown in Figure 4-4

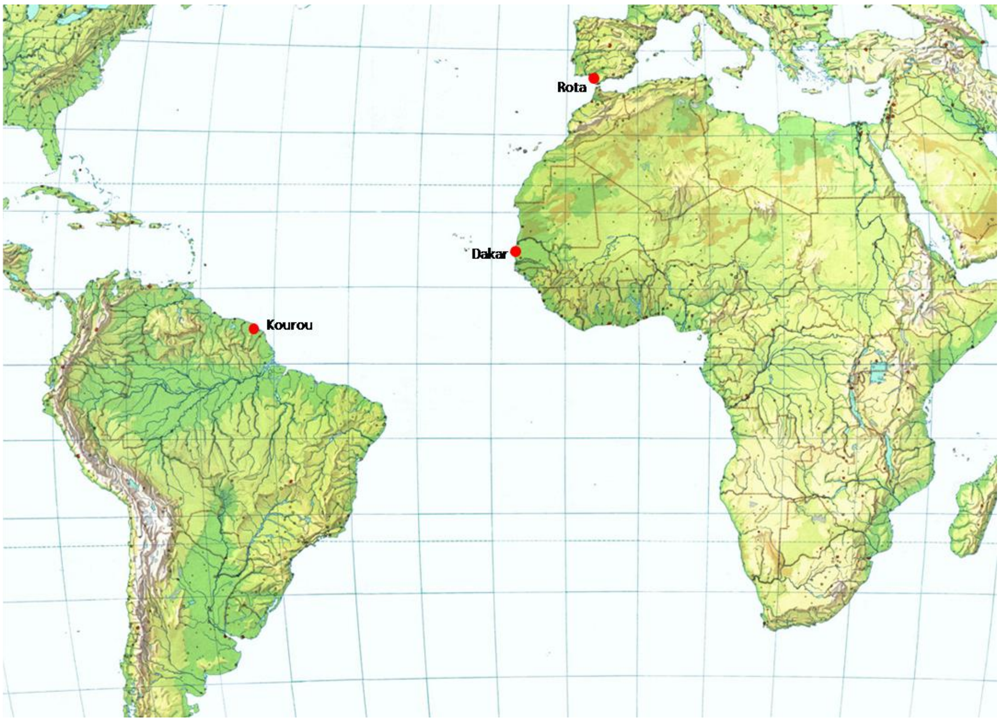

Figure 4-4: Preferred nominal Landing Sites

5 REFERENCE CONFIGURATION OF A HIGH L/D VEHICLE FOR EARTH RE-ENTRY

5.1 REFERENCE VEHICLE

In the past various re-entry vehicles have been proposed and used. From these vehicles the capsule principle has been used most often and has shown to be a very reliable re-entry vehicle. Now looking at these conventional hypersonic re-entry vehicles like capsules or the Space Shuttle the following characteristics uphold:

- A rapid and steep re-entry
- Critical aero-thermal conditions
- Need for massive thermal protection systems (TPS)

The improvement by the use of a high Lift-to-Drag vehicle can be seen in the following:

- Reduction of acceleration forces and thermal loads
- Increase of downrange & crossrange capability and maneuverability by a long gliding phase which allows a much wider “re-entry window”

During the study different High Lift-over-Drag vehicles, like waveriders and the OHB Space-Plane were considered and compared with the previously flown vehicles Apollo, Soyuz/Zond X-38 and Space Shuttle as well as vehicles under development like ORION and a biconic capsule.

Based on the preselected, most potential vehicle for this kind of re-entry – the Low-Risk-re-entry vehicle Spaceplane LR-L/LR-M, several updates were investigated and resulted in the reference SpacePlane PHOEBUS-HL-3A. This is a vehicle with an innovative hot structure concept equipped with new materials like UHTC and innovative design with sharp leading edges (see Figure 5-1).

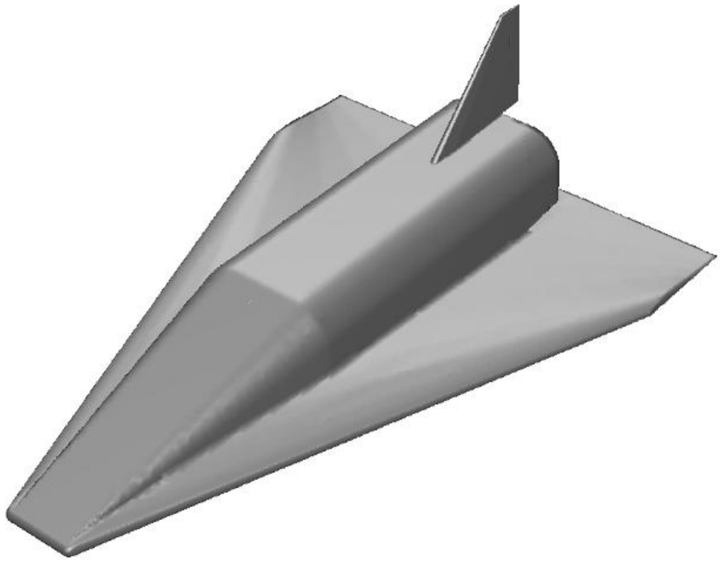

Figure 5-1: Reference SpacePlane PHOEBUS HL-3A

It has a mass of about 5t (without Resource Module) with a length of about 11.6 m and a width of about 8.3 m. The sharp leading edges have radii of about 5 to 10 cm. The wingload is about 80 kg/m². Materials selected for the vehicle are:

- Ultra High Temperature Ceramics (UHTC): for ultra high temperatures components like wing - and fin leading edges [T > 1900K])
- C-SiC: for windward areas like vehicle windside structure and control surfaces (rudder, elevons and body flap) [1300K<T<1900K]
- SiC-SiC for skin and leeward areas (vehicle upper side) [1000K<T<1300K]
- Metallic skin (e.g. Superalloys) or light Flexible External Insulator panels: for leeward areas of the vehicle fuselage and wings with relatively low temperature [T< 1000K]

The vehicle is designed for a crew of three and a flexible Resource Module concept for different missions.

The design reflects a good combination of the structural – and thermal requirements. Furthermore the operational advantages like landing on a conventional runway (< 3km length, Airplane like behaviour) and mission flexibility due to large down- and crossrange capability are realized.

Various different re-entry vehicles were designed in the past and are even under investigation today. Looking at the proposed PHOEBUS HL-3A vehicle it can be said that the system has a number of highly attractive characteristics which makes this concept the preferred basis for future re-entry vehicles.

- Innovative thermal protection system (Hot Structure Concept & TPS) which is mainly localized at the tips of the fuselage/wings/control surfaces.
- Low pressure forces and decelerations, in particular during the highest heat fluxes
- Controllability (pilotability) of the vehicle along the entire flight path possible
- Low landing speed (beneficial for use of standard runways and for abort at launch), associated to the low wing loading and to the streamlined vehicle shape (any airport can serve as backup).
- A very large landing footprint due to the long re-entry duration. Downrange of the order of 55000 km and cross ranges of the order of 3800 km will guarantee a wide choice of landing spots.
- No black out in the radio-communications to ground and to satellites because a thick plasma sheath around the vehicle is not formed.
- No parachute system (main & drogue) or critical retrorockets are used.
- Less complex structure then other winged re-entry solutions (e.g. Space Shuttle)

5.2 SYSTEM PERFORMANCE

5.2.1 REFERENCE RE-ENTRY TRAJECTORIES

A normal return from a Moon mission reflects a superorbital leg as well as a sub-orbital leg. As such, the return from a Moon mission envelops also a typical return from a LEO mission. For this reason more emphasis has been put onto typical return missions from a Moon mission, which reflects into 3 different possible scenarios compared to one for a LEO return.

5.2.1.1 Reference trajectory from LEO

The reference missions for re-entry from LEO foresee crew return from ISS and re-entry from lunar transfer orbit (LTO). In general, the re-entry trajectories from LTO include a super-orbital leg and a sub-orbital leg, thus enveloping also typical re-entry trajectories from LEO. For this reason the attention has been focused on re-entry from Moon, and only one possible re-entry trajectory, from the ISS orbit to the Kourou spaceport, has been identified.

For this return trajectory the chosen reference trajectory stays exactly within the boundaries predefinded for this return. The maximum heat flux at the stagnation point stays within the limit of 0.7 MW/m^2 and an angle of attack of 25° is uphold. Due to the high Lift-over-Drag ratio and by adjusting its AoA it can remain at an altitude of 80 km for a long time (see *Figure 5-2*). Finally the accompanying ground track of the reference trajectory from LEO is shown in Figure 5-3.

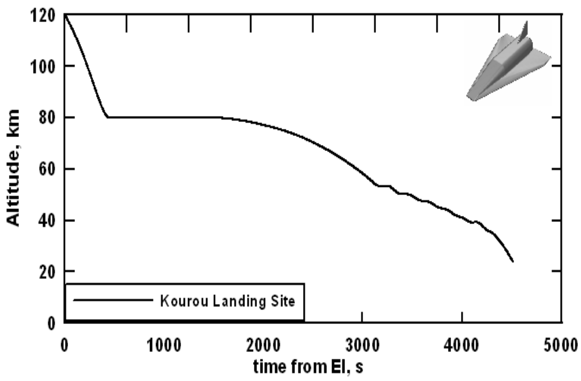

Figure 5-2: Nominal re-entry trajectory from LEO mission: Altitude versus time

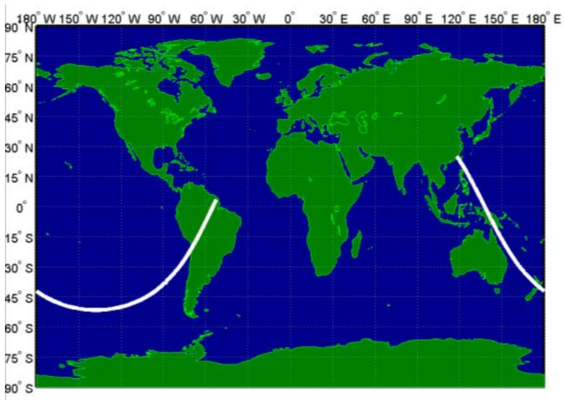

Figure 5-3: Ground track nominal re-entry trajectory from LEO mission for a landing at Kourou

5.2.1.2 Reference trajectory from the Moon

For re-entry from Moon, three different trajectories have been identified, in order to reach our three landing sites, namely our nominal one Kourou Spaceport, and the other two Rota and Dakar. But the trajectories are almost coincident in the altitude-velocity plane, because the same strategy is adopted. The chosen trajectory stays accurately within the preset boundary limits. The maximum heat flux at the stagnation point stays within the limit of 2.0 MW/m^2 and the equilibrium glide boundary of attack of 40° is uphold.

The initial AoA=33° value has been chosen because it is the lowest value of AoA allowing the aerocapturing without exceeding the thermal boundary in order to reduce the aeroheating of the PHOEBUS windside. In the Figure 5-4 the nominal re-entry trajectories can be seen against altitude. From this it can again be seen that due to the high Lift-over-Drag ratio the chosen concept and by adjusting its AoA it can remain at an altitude of 80 km for a long time. The ground tracks of these trajectories are shown in Figure 5-5.

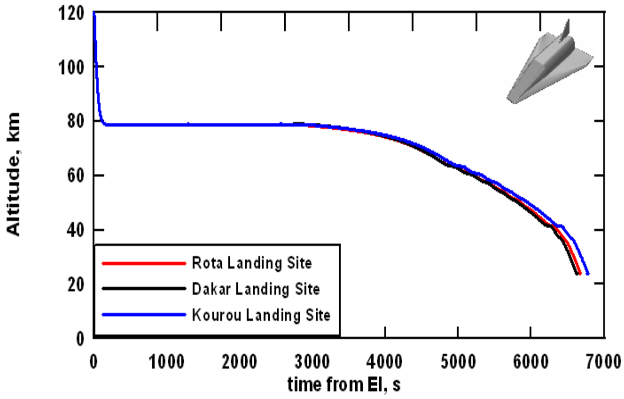

Figure 5-4: Nominal re-entry trajectories from Moon mission. Altitude versus time.

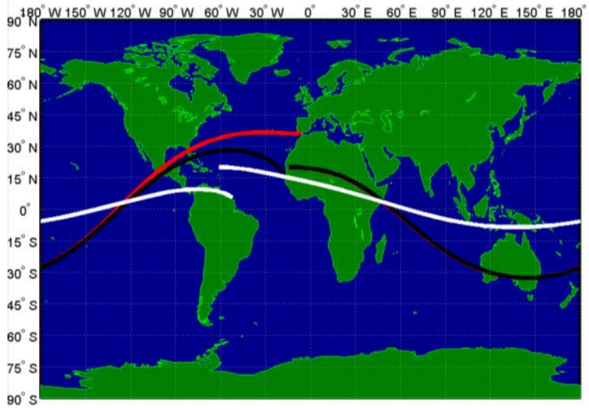

Figure 5-5: Nominal re-entry trajectories from Moon mission to Rota (red), Dakar (black) and Kourou (white). Ground tracks.

It must be pointed out that the trajectories shown in Figure 5-4 and Figure 5-5 are not unique to achieve the desired landing point. By adjusting the AoB and AoA strategy different solutions can be obtained.

5.2.2 MANOEUVRABILITY DURING FLIGHT

To be able to fly according to these boundaries and the predeveloped nominal trajectories the proposed re-entry vehicle has to poses good manoeuvrability and landing coverage. For this reason the vehicle was designed to have a high Lift-over-Drag ratio and is foreseen to have the control surfaces shown in Figure 5-6:

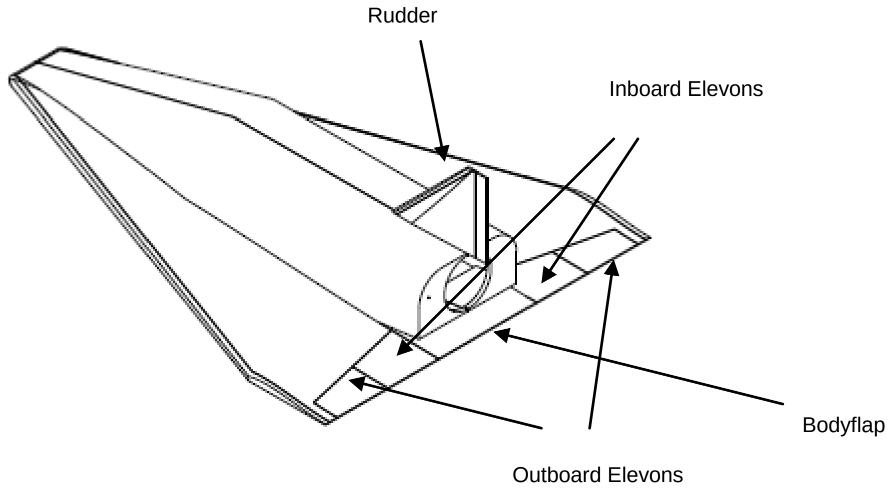

Figure 5-6: Control surfaces PHOEBUS HL-3A

The proposed PHOEBUS HL-3A re-entry vehicle has a high Lift-to-Drag ratio of 2.9, such that it can glide at high altitudes for a long time, during which it reduces its energy, before it lands on Earth. This capacity generates a very big downrange capability. In addition, with the help of its control surfaces and the accompanying of angle of bank adjustments, the vehicle is capable of attaining a considerable crossrange. These two points are a major advantage over capsule like re-entry vehicles and other low Lift–over-Drag vehicles which only have a very limited down and crossrange and as such a rather steep re-entry path.

5.2.3 POSSIBLE CROSSRANGE AND DOWNRANGE

For the chosen HL-3A configuration a detailed analysis was performed to obtain the maximum possible crossrange and the minimum and maximum downrange, taking into account a maximum allowable heatflux of 2.0 MW/m^2 in the stagnation point and a maximum peak deceleration of 4 g. In particular, for the configuration HL-3A for both a return from the Moon and from a LEO mission the minimum and maximum downrange as well as the minimum and maximum crossrange was evaluated. For comparison the different maximum values are also presented against the other re-entry vehicles (see Table 5-1).

Vehicle / Parameter	Soyuz / Zond	Apollo	ORION (CEV)	Biconic	Space Shuttle	X-38 CRV	Waverider	LR-L	LR-M	PHOEBUS HL-1A	PHOEBUS HL-2A	PHOEBUS HL-3A
Downrange / crossrange (LEO) [km]	2500 / 80	N/A	4500 / 200	5500 / 350	10000/ 1300	13000 / 1100	13000 / 3100	36000 / 2700	30000 / 2200	30000 / 2200	36000 / 2700	36000 / 2700
Downrange / crossrange (Moon) [km]	9000 / 300	3700 / 120	13000 / 500	28000 / 500	N/A	29000 / 2000	N/A	55000/ 3800	45000 / 3200	45000 / 3200	55000 / 3800	55000/ 3800

Table 5-1: Down-- and crossrange of the different re-entry vehicles

From this table it can be seen the proposed re-entry vehicle PHOEBUS HL-3A has superior maximum down and crossrange capabilities in comparison to previously flown vehicles, but also in comparison to the newly being developed CEV vehicle. Furthermore, these capability from a Moon mission and LEO mission provides very high flexibility in choosing its landing side, for nominal return and in contingency case.

5.2.4 LANDING CHARACTERISTICS PHOEBUS HL-3A

The PHOEBUS HL-3A concept can theoretically land on every airport available on Earth. As the vehicle lands with a rather low landing velocity (~50 m/s) and due its low mass (~5000 kg) the landing loads will be quite low (significantly lower than with a Boeing 747) on the runway hereby generating a big range of possible runways.

Due to the lack of a high Lift-over-Drag ratio and the absence of significant control surfaces, earlier missions with capsules (e.g. Apollo, Zond and Soyuz) and the future CEV lack this flexibility in landing. Furthermore the Space Shuttle, which does land on a landing strip, requires a substantional runway length due to its high landing velocity.

5.2.5 RE-ENTRY THERMAL LOADS

An important aspect of re-entry is the induced thermal loads. To make the thermal loads more transparent, again a comparison is made with previous flow vehicles and the currently under development CEV. For this the stagnation point temperatures have been determined by radiative equilibrium assumption with an emissivity value of 0.8. The results can be seen in Table 5-2 and Table 5-3 below. For the PHOEBUS HL-3A, the presented values are for a nominal landing at the Kourou Spaceport.

RE-ENTRY FROM LEO		
Vehicle	**Maximum Heating rate [MW/m^2]**	**Max St. Temperature [K]**
Soyuz	0.65	1950
CEV	0.3	1600
Flattened	0.6	1900
SS Orbiter	0.57	1880
X-38 CRV	0.75	2000
Waverider	1.1	2220
PHOEBUS HL-3A	0.7	2000

Table 5-2 Comparison of Heating Performance from LEO

RE-ENTRY FROM MOON		
Vehicle	**Maximum Heating rate [MW/m^2]**	**Max St. Temperature [K]**
Zond	2.6 + 4.7	3550
Apollo	2.2 + 4.7	3510
CEV	1.4 + 4.2	3300
Flattened Biconic	0.33	2100
X-38 CRV (Lifting body)	0.90	2400
PHOEBUS HL-3A	1.9	2500

Table 5-3 Comparison of Heating Performance from Moon

For a return from LEO, where the convective heat input will be the dominant heat load factor, it can be seen that capsules have the lowest maximum heating rate due to the bluntness of the configuration. In comparison, the high Lift-over-Drag vehicle Waverider, with relatively sharp wing leading edges and fuselage tips, exhibit maximum heat fluxes in the excess of 1 MW/m2, which will require special TPS materials to secure structural integrity. Due to the innovative re-entry strategy, the PHOEBUS HL-3A vehicle can assure, even though it is equipped with sharp cylindrical nose, a maximum heat flux of 0.7 MW/m2 which is in the same range as the X-38 vehicle.

For a return from a Moon mission, the radiative contribution to the heat flux will become more dominant. In the case for very blunt configurations this contribution becomes even higher than the convective (see the split of convective (left) and radiative (right) contribution in Table 5-3). For the PHOEBUS HL-3A as the nose and the wing leading edges curvature radius are small and the vehicle gently decelerates at relatively high altitudes, the radiative contribution is negligible. For the other vehicles, the radiative contribution is negligible and as such only the convective value is presented in the Table 5-3.

Summarizing it can be said that the proposed PHOEBUS HL-3A vehicle has a very moderate stagnation heat flux for LEO, and for a return from Moon it is not penalized by a large increase in thermal load due to radiative heating, which the capsule type re-entry vehicles exhibit. In general it can be said that for the chosen concept PHOEBUS HL-3A with sharp leading edges, the flown trajectory induces high stagnation point temperatures and very localized in comparison to blunt re-entry capsule. For a return from LEO, when flying with a limited AoA this means the high thermal loading is very localized with accompanying local high temperatures, but these temperatures will reduce very fast when moving to the back of the vehicle, this in comparison to the Space Shuttle which flies with a much higher AoA. The result for the Space Shuttle is that the induced heat flux to the outer body reduces much slower in comparison to the PHOEBUS vehicle when moving back along its length (and as such the present local outer surface temperatures).

For a return from a Moon mission, the same philosophy is applicable. Only for the first part of the re-entry, the PHOEBUS has to fly with a significant AoA to perform aerocapture into the Earth’s atmosphere (AoA of 33°) which results in more spread out thermal loading. However, this condition is only uphold for a short period, after which the PHOEBUS vehicle continues with very low AoA, which again guarantees a quick drop in heat flux and accompanying temperatures.

The result of the more localized high heat loads at the forward area of the vehicle generates the possibility to apply the heavy materials that can withstand these (e.g. UHTC for temperatures > 1900 K) only over a small area at the front and at the leading edges, and that for the more rearward parts lighter materials can be used.

An important aspect of the re-entry of the PHOEBUS vehicle is that it slowly reduces its energy at high altitudes and as such takes more time for its re-entry. In general a high value of the peak heat flux may be better tolerated than a lower heat flux that lasts much longer. However due to an innovative build up of the thermal system based on the concept of hot structures, also aspect can be coped with. The principle is based on that heat entering the vehicle is stored in the whole structure until the global radiative equilibrium is achieved, i.e. the integral of surface heat flux is zero at each instant of time. In this condition the heat load is zero. An integrated approach based on the knowledge of re-entry trajectories, materials and thermal structures configuration is necessary to evaluate the effective heat load entering the vehicle. The aerothermal design must be accomplished with a trial and error procedure based on the computations of the temperature of the vehicle structure along the trajectory until the trajectory, materials and structural configuration requirements are satisfied. A very rough initial guess on the temperature assumes that the local radiative equilibrium temperature is achieved at each surface point (net heat fluxes equal to zero).

Furthermore it must be said that the materials envisaged for the PHOEBUS vehicle (leading edges, hot structures and high temperature insulator) are characterized by a relatively low TRL at the moment. However, due to intensive research the TRL of these materials is can be increased considerable within the upcoming years.

5.2.6 MECHANICAL RE-ENTRY ENVIRONMENT

The maximum occurring g-loads are in the range of 1 g for a return from both a LEO and a Moon mission. Due to the high energy return from a Moon mission (an entry velocity in the range of 10.5 km/s) it can be said that the deceleration during the aerocapture after the first leg of the entry trajectory is significantly higher than with a LEO re-entry where the re-entry velocity is approximately 7.5 km/s. For a comparison to other re-enry vehicles, the maximum occurring g-loads for the PHOEBUS vehicle are presented against other re-entry vehicles in the table Table 5-4 below.

RE-ENTRY FROM LEO	
Vehicle	**Peak Deceleration G's**
Soyuz	3.1
CEV	3
Flattened biconic	2
SS Orbiter	2
X-38 CRV (Lifting Body)	1.2
Waverider	1
PHOEBUS HL-3A	~1

RE-ENTRY FROM MOON	
Vehicle	**Peak Deceleration G's**
Zond	7.8
CEV	4
Apollo	8
Flattened biconic	1.4
X-38 CRV (Lifting Body)	1.2
PHOEBUS HL-3A	~1 – 1.1

Table 5-4 Comparison of maximum occurring g-loads during re-entry

From the Table 5-4 it can be seen that the proposed PHOEBUS HL-3A vehicle has for both a return from a LEO mission as for the return from a Moon mission the lowest maximum deceleration forces of all vehicles compared when flying its nominal trajectories.

The induced dynamic pressures during the return from LEO and from a Moon mission for the nominal trajectories are very similar to the deceleration profiles which were presented earlier. The first peaks of the dynamic pressure corresponding to the aerocapture manoeuvre are less than 500 Pa for LEO re-entry and about 1000 Pa for Moon reentry. The maximum values for the dynamic pressure are in the range of 5000/5500 Pa from LEO and 3500 Pa for a return from the Moon and occur in both cases at lower altitudes, when the aerothermal loads strongly decrease due to the reduced kinetic energy of the vehicle

In the Table 5-5 below a comparison can be seen of these dynamic pressures is presented with respect to other re-entry vehicles.

RE-ENTRY FROM LEO	
Vehicle	Peak Dynamic Pressure kPa
Soyuz	22
CEV	11.5
Flattened biconic	9
SS Orbiter	11
X-38 CRV	8
Waverider	3.4
PHOEBUS HL-3A	5.5

RE-ENTRY FROM MOON	
Vehicle	Peak Dynamic Pressure kPa
Zond	58
CEV	31
Apollo	32.5
Flattened biconic	8.6
X-38 CRV	8.2
PHOEBUS HL-3A	3.5

Table 5-5 Comparison of dynamic pressure during re-entry

From the comparison between the imposed loads on the PHOEBUS HL-3A and on the other vehicles it can be seen that for a nominal trajectory the loads are very low. When the PHOEBUS vehicle does not fly its nominal trajectory but follows the trajectory of the maximum allowable heat flux (see Figure 5-7) it can be seen that the involved dynamic pressure increases a lot to equivalent values to a return with the CEV or Apollo capsule from lunar missions.

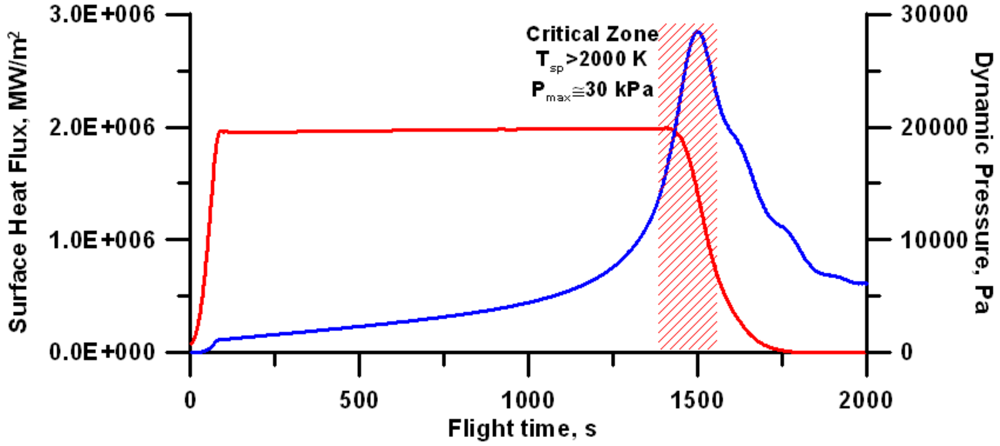

Figure 5-7: Mechanical and thermal loads along the maximum heat flux trajectory

From the last comparison, it is highly desirable if the re-entry vehicle is able to fly along a specific trajectory (e.g. the nominal trajectories for LEO and Moon missions) to keep the dynamic pressure loads on the structure to low values.

5.2.7 SAFETY ASPECTS

For the designed re-entry vehicle it has been documented in TN 4-3 that for its launch two feasible possibilities exist, namely on top of an appropriate launcher (Ariane 5) and via a heavy lift aircraft launch.

Looking at its safety aspects for a nominal launch with an appropriate launcher the proposed re-entry vehicle, PHOEBUS HL-3A, has a very big advantage over capsules and over low Lift-over-Drag vehicles like the Space Shuttle. This aspect can be seen when a mission abort has to be performed just after launch. As the PHOEBUS HL-3A vehicle has such a high Lift-to-Drag ratio (2.9), it will be able to return to the landing site after a significant longer time (bigger distance) after launch then other lower Lift-to-Drag vehicles due to its very good gliding capabilities/properties. Furthermore, the PHOEBUS HL-3A has a significantly lower (minimum) landing velocity, which will enable it to land also during early abort scenarios where the Space Shuttle would not be able to safely land. What must be noted at this point is that for the launch of our vehicle no crew escape system is foreseen which is being used in the very early stages of the launch. This is an aspect has to be studied in more detail during a follow-on study.

From the previous subchapter 5.2.3 it could have been seen that our proposed re-entry vehicle has a very large cross and downrange capabilities. Due to these, the PHOEBUS re-entry vehicle has a big range of landing possibilities which increases the survival changes of the crew considerable. Additionally, due to a very limited landing velocity the number of possible landing sites is furthermore drastically increased. These aspect of landing on a normal landing site can be seen as big positive point for the PHOEBUS re-entry vehicle with respect to capsules which normally land in a rather big designated area (On land for the Soyuz & CEV, in the sea for Apollo) where recovery may consume much more time which may be very problematic in case of an injured crew.

A point that is a major issue for the current return of the Space Shuttle (which is also applicable for capsules) is the time it requires before it can initiate its re-entry procedure due to its limited re-entry window (due to only a limited number of possible landing sites/areas). Due to the large cross and downrange capabilities of the proposed re-entry vehicle this point is also far less an issue, and much more flexibility exists for the re-entry. Especially in contingency cases (e.g. injured crew) this increased flexibility in return to Earth is a major advantage. In general it can be said that due to the just mentioned flexibility, the landing possibilities for the proposed re-entry vehicle.

Looking at the different mechanical loads which the re-entry vehicle is subject to it can be said that again the PHOEBUS re-entry vehicle is a very good option concerning the crew safety. With respect to the maximum deceleration loads it could have been seen from the previous subchapter 5.2.6 that these are very low in comparison to the other re-entry vehicles. A factor 3 with respect to SOYUZ return from LEO and even a factor 8 with respect to a Zond return from Moon. As such a return for the crew is very pleasant with only limited deceleration loads and therefore a big plus point for the proposed vehicle. To accomplish these very low deceleration loads, of course the PHOEBUS vehicle will take more time to return to the Earth's surface, but as the re-entry time is neglectable in comparison to mission lengths this may not be seen as a negative point. (In case of an injured crew the PHOEBUS vehicle can return back to the Earth's surface in a timely manner when flying a trajectory with a minimum downrange). With respect to the induced thermal loads when returning from a LEO or Moon mission, it was pointed out that these are very localized and only on a limited area with respect to capsules and with respect to the Space Shuttle. In addition the PHOEBUS will be manufactured from a much smaller number of thermal critical components (sharp leading edges) w.r.t. the Space Shuttle (Heat shield of circa 50000 tiles). With regards to safety these points are also considered as a positive point. The PHOEBUS vehicle has due to these mentioned points a much smaller number of components which will induce a total loss of vehicle when structural failure would occur at these components.

As a last point it can be said that it is foreseen that our vehicle will be flying autonomously such that in the case of unconsciousness/incapacitated crew the vehicle will be able to land as would be the case with a capsule.

What must be noted is that due to its more complex nature (winged configuration) in theory also more can go wrong during re-entry. As such, a less complex structure, as a capsule, has an increases safety aspect from this point of view. Moreover it must be said that the longer the re-entry takes the more time there is for accidents to happen. However, due to all the other safety points that were just mentioned, it must be concluded that a crew would be safer from a total mission point of view with the PHOEBUS HL-3A re-entry vehicle in comparison to earlier flow capsules (Apollo, Zond) and the currently under development CEV.

6 GUIDANCE PERFORMANCES FOR A HIGH L/D VEHICLE

6.1 GUIDANCE AND CONTROL

G&C algorithms are mostly compliant with the majority of requirement that basically presents the performances for the baseline scenario: Landing at Kourou

Nevertheless, for the other mission scenarios (nominal and contingency cases) reduced performances are experimented in terms of final downrange accuracy for landing at Rota and for the shorter contingency landing at Kourou.

Moreover, it has been reported that the shorter contingency scenario to Kourou exceeds the maximum g-load established to 4. However this is only a fictitious figure generated by the 4 DoF simulation environment.

As shown in Figure 6-1 in fact, this occurs only during a few seconds when the algorithm passes from 33 deg AoA to the second phase flown at 20 deg AoA. When introducing a more realistic attitude controller in the loop, this situation will certainly disappear. For this reason this figure is not reported as “not compliant” in the corresponding column and no major emphasis is put on it.

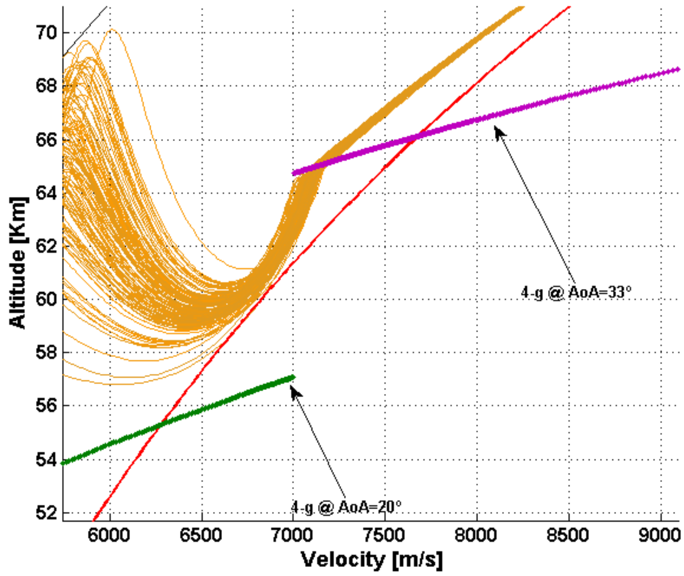

Figure 6-1: Monte Carlo: Altitude/Velocity – Detail on targeting

The problem related with the lack of downrange accuracy is deemed more important and a series of consolidation issues have been identified and are briefly discussed here after.

These points have to be regarded as strong recommendations to be taken into account for future maturation of the G&C re-entry algorithms for Phoebus vehicle.

6.1.1 DOWNRANGE-CROSSRANGE COUPLING

The targeting algorithm works by solving a two-point boundary value problem in the longitudinal channel, in order to find two parameters that characterize a linear bank angle control law that results in a trajectory that connects the downrange and altitude at targeting to downrange and altitude at TAEM speed. To do so, the distance to the target is computed and the objective downrange-to-go, that is, the downrange from current position to TAEM that needs to be traveled, is assumed to be equal to the distance to TAEM.

This is a fair assumption when the heading at targeting is directed towards the target, that is, no significant crossrange corrections need to be performed during targeting, except for periodic bank angle reversals to keep the groundtrack a straight path. However, when a large downrange needs to be corrected after targeting, the groundtrack will be curved, as a result of banking mainly into the direction of the target. Due to this, the longitudinal guidance will command vehicle to TAEM altitude and velocity where traveling the prescriped downrange, which will fall short of the necessary downrange to get to the prescribed distance to target.

Figure 6-2 illustrates this effect in groundtrack.

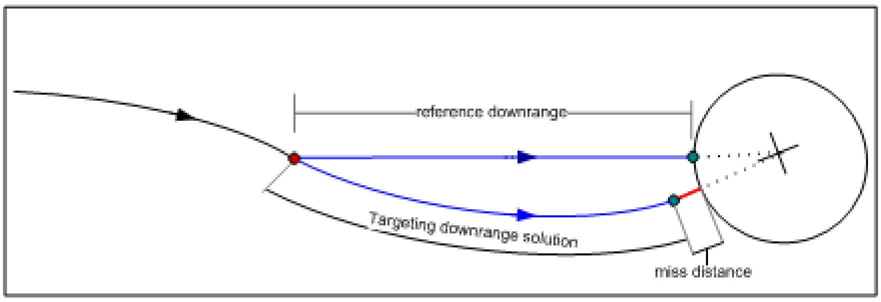

Figure 6-2: Groundtrack for same travelled distance, different heading errors at targeting

Whereas this crossrange-downrange coupling after targeting was seen to be negligible in cases of initial nominal crossrange below 1500 Km, where crossrange has been corrected up to targeting (Dakar scenario and also Kourou, to a level), this coupling caused systematic miss distances in the case of Rota, where a large initial crossrange exists upon targeting.

An improvement to be considered in the algorithm is, since the targeting function already includes a 4DOF propagator, to include simulated lateral guidance internally, and optimize the final distance to target instead of traveled downrange from targeting.

6.1.2 BANK ANGLE REVERSALS

The current lateral guidance scheme works independently from the longitudinal guidance. It issues a bank angle reversal whenever the crossrange crosses a limit, which is dependent on distance to target and velocity. That way, whenever the current orientation of the bank angle is diverting the spacecraft too much from its correct heading, it is reversed in the opposite direction. During prototyping and testing of the algorithm, this was seen to cause a high number of bank angle reversals, in the order of 10. This is undesirable because, when applied to a full 6DOF bank angle reversals will not change instantaneously from one quadrant to the other, affecting, while changing, the longitudinal path.

In order to reduce the number of bank angles, the boundaries can be widened up to targeting and a single or double bank angle reversal strategy can be thought off, where the search function in targeting will compute the right moment in the guidelines (the guidance logic envisaged for the X-33).

6.1.3 DOWNRANGE CONTROL UNTIL TARGETING

The longitudinal algorithms used in the first two phases of the reentry issue bank angle commands to control the amount of lift in the vertical direction. While in the first phase the tracked variable is altitude, in the second heat flux, in the form of a velocity-altitude correspondence is tracked. Up to 20 000 Kms are travelled in this first phase, with no downrange control being used. The rationale is that since one follows the nominal altitude, and reference drag is assured by following the nominal angle of attack history with respect to velocity, little to no downrange perturbations will occur, and, if so, they are corrected at targeting.

However, given the long paths to be travelled, and the high uncertainty in atmospheric density at these altitudes (and to a level, in aerodynamic database), the drag history experienced during the constant altitude phase can differ significantly from nominal, and lead to downrange errors that stress the targeting to its limits.

Because of a number of physical constraints, the most direct way of compensating for drag differences, which is adjusting the drag coefficient through angle of attack adjustments, is not a possibility for the guidance scheme. Since, due to trimability issues and alike, angle of attack follows a nominal with respect to Mach history, drag can only be used to compensate perturbations (and perturbations in downrange) by issuing bank angle commands to change the amount of vertical lift to rise or fall in altitude and thus density, which is proportion to drag.

An improvement of the algorithm in the first phase can thus be the issuing, at very low frequencies, of off-nominal altitudes to compensate errors in downrange. If downrange needs to be compensated by travelling faster (relatively to nominal), a higher reference altitude should be followed so that drag is lower, and vice-versa.

6.1.4 CAPTURE IN OFF-NOMINAL CONDITIONS

Some of the extreme conditions for capturing Lunar reentry, in terms of entry speed and flight path angle are physically impossible to tackle, even with an angle of attack for maximum drag and a bank angle of 180º for maximum lift in the downwards directions. These physical conditions are mainly due to:

- Atmospheric density can vary by up to 30% at the reference altitude of 80 Km and from above 90 Km can vary up to 50%. A less dense atmosphere implies proportionally less drag acceleration.

- Imprecision in initial flight path angle and entry speed can also pose increased difficulty to capture, as seen in Figure 6-3: a less steep flight path angle or a lower reentry velocity can take the path to above actuation limits to capture. On the other hand higher velocities and steeper flight path angles take the trajectory closer or over the heat rate limitations (Figure 6-4).

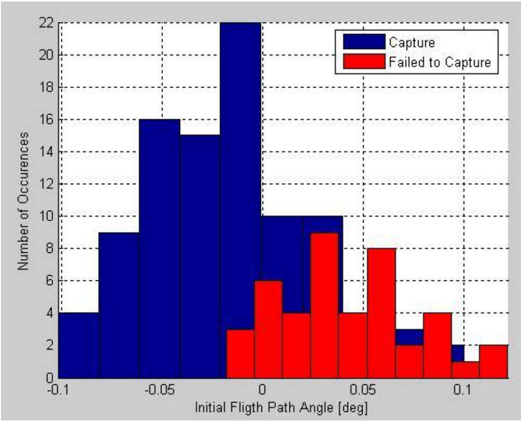

Figure 6-3: Perturbation in flight path angle effect on capture success for a Monte Carlo run.

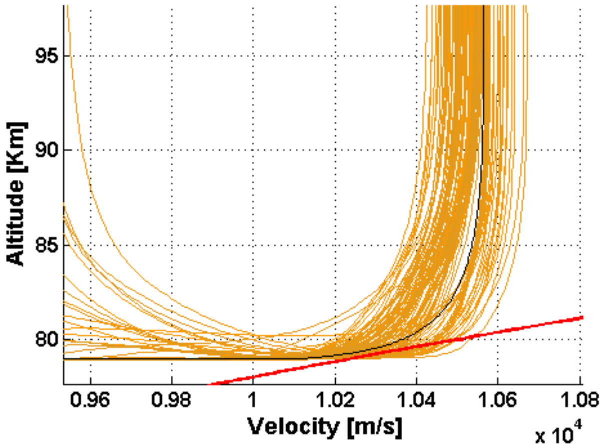

Figure 6-4: Reentry from perturbed initial conditions

The guidance algorithm at this point issues bank angle commands to track a prescribed altitude with a second order behavior whose damping and natural frequency are tuning parameters. By improving the tuning of these parameters one can avoid, to a level, an overshoot in the downwards direction, which might lead to exceeding the maximum allowed heat flux, and in the upwards direction, which, in a less dense atmosphere, would lead to failure to capture. Another workaround would be to issue an initial heat rate following algorithm. At the high velocities encountered during capture, the fact that one is flying close to the upper boundary limit for capture, in altitude, is also an issue since even a small rise above that level (in an overshoot, due to off-nominal conditions or due to a high damping ratio) takes the vehicle to less dense atmosphere where control authority decreases and may not suffice.

In summary, due improvements for dealing with Lunar reentry capture in off-nominal conditions are:

- Careful tuning of the second-order-behavior parameters damping and frequency.
- Using a dedicated guidance phase for capture, with the heat rate following algorithm to tackle heat rate constraints directly at the early phase

- Not a GNC improvement, but an input to trajectory generation: have the constant altitude following phase 5 kms below current value. Having reference trajectories close to system limits leaves little space for dealing with off-nominal conditions

- In order to better assess performance in capturing, the expected precision in flight path angle and velocity and EI needs to be derived and provided to do a GNC analysis.

To be noticed that this only applies for Lunar returns, since LEO return velocities and flight path angles don't imply a full lift down for capture

6.2 NAVIGATION

Navigation performance assessed for the PHOEBUS vehicle are very close to the ones assessed for the ARD with a similar navigation function. This represents a validation for the NPM designed and implemented for the PHOEBUS vehicle.

ARD performances exceed significantly PHOEBUS accuracy in what regards the latitude and especially the longitude that turns in a higher local horizontal error.

In what regards the global horizontal error, value reported is the minimum accuracy available in the flight. This accuracy improves when reaching the TAEM to about 6 km.

The local horizontal accuracy is completely driven by the accuracy on latitude and longitude. This should be improved when improving

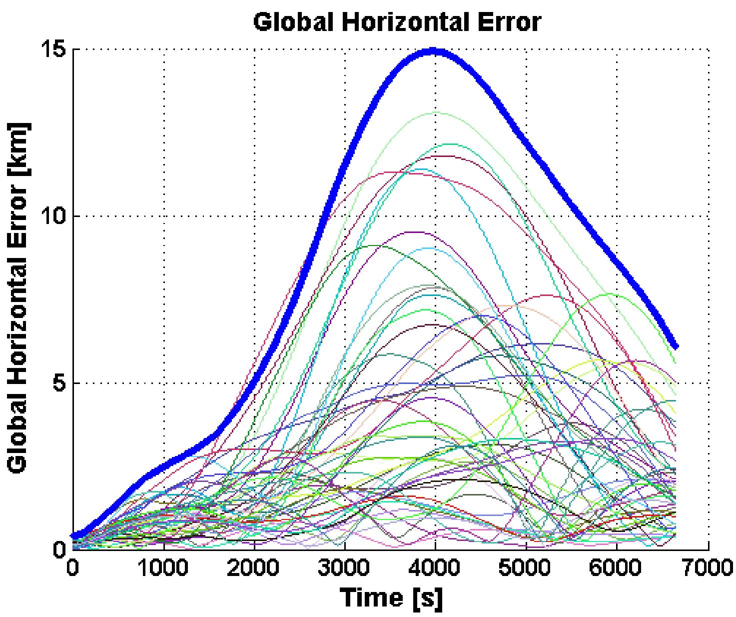

Figure 6-5 Global Horizontal Error

However, better navigation performances for the ARD vehicle were, indeed, expected due to a twofold reason:

- Shorter re-entry:

  The ARD re-entry phase took around 10 minutes. This shorter time limited the effect of the vertical channel instability. The re-entry time was basically corresponding with the time constant of the vertical channel divergence in the INS. This contribute to the better performance seen for the ARD

- Kalman Gain Updating:

  Pre-computed Kalman gains, scheduled versus altitude, were stored on board the ARD. These allow updating the altitude in the INS using a Kalman filter scheme. This not only improves the performance for the altitude, but also has an impact on the local horizontal accuracy.

  This is due to propagation within the INS (Inertial Navigation System) that is carried out in an inertial reference system created correlation between the altitude and the local horizontal position.

  The measurement updating though a Kalman filter is here considered an important issue to be addressed in future phase of the PHOEBUS vehicle design. A part for the performance (already accurate), it shall increase the robustness of the navigation scheme and its implementation should be considered for a more mature design.

7 STUDY SYNTHESIS & RECOMMENDATIONS

In this chapter the outcome of all work packages of this study is summarized and reasonable next steps needed for more detailed understanding of the feasibility of such a high L/D vehicle are described.

7.1 STUDY SYNTHESIS

The task of this study required a detailed understanding and investigation of the difference between the innovative re-entry strategy of a high lift-over-drag earth re-entry vehicle compared to the re-entry strategies of conventional vehicles like capsules, biconics, lifting bodies, the Space Shuttle and waveriders.

The analysis and comparison of the different entry strategies led to the conclusion, that the high L/D re-entry strategy has a lot of potential for enhancements of the flight performances and mission flexibility. This is founded especially by the noticeable increase of the downrange and crossrange which allows a wide range of flexibility wrt entry windows and landing site reachability. At the same time a reduction of the risks for the crew and vehicle can be realized by the use of a re-entry strategy with a long glide phase at high altitudes and low load factor.

The specified most potential high L/D vehicle PHOEBUS HL-3A achieves the requirements for LEO - and also Moon mission return with a crew of three, by using innovative design solutions like slim wing, sharp leading edge structures and high-tech materials like UHTC. Because the focus of this study was set to the guidance and control aspects without deeper analysis of the complete vehicle design and its thermal analysis these aspects couldn't be investigated in more detail. But this has necessarily to be regarded for a better appraisal of the feasibility, performance and limitations of such a concept.

Nevertheless, after a detailed analysis of the flight mechanics with all the necessary aspects like trimmability and controlability during all flight phases, the upgrade of the PHOEBUS shape versions (from HL-1A to HL-3A) leads to shape with excellent down- and crossrange performance and compared to conventional re-entry vehicles with low structural loads.

Also the analysis of the aero- and aerothermodynamic loads showed, that the PHOEBUS HL-3A hot structure concept fulfills the complete requirements, which are made by such a high L/D re-entry trajectory.

Apart from the G & C limitations related to the downrange accuracy of several contingency cases explained in Chapter 6 also the guidance and control algorithms are fully compliant to the requirements given by this study.

However the study shows essentially positive aspects also critical topics shall not concealed. As one of the most critical part of the feasibility aspects is the Technology Readiness Levell (TRL) of the manufacturing and producibility of UHTC structures. Already existing UHTC materials are currently achieves only the prototyping level TRL 5. The producing industry assesses a TRL6 - 9 in the range of 15 Years from now. Among this, also the interconnection of the different hot structures and the varying coefficient of expansion shouldn't be underestimated.

7.2 RECOMMENDATIONS FOR NEXT STEPS

During the High-Lift study, the big influence of the thermal loads which are affecting the structure was identified. The feasibility of the vehicle design depends on the availability of suitable materials and producibility. Because the study focus was on the re-entry strategies using high lift-over-drag ratios as well as the guidance and control techniques a detailed thermal analysis of the structure was not foreseen. However, for the further steps it is mandatory to analyze the effectively occurring loads to the structure to find the application limitations.

Also some main concept evaluations are necessary to confirm a maintainable vehicle design. This is especially a more detailed look onto the chosen structure materials. A thermal analysis is necessary to show the feasibility of the PHOEBUS structural concept and to properly define the structural design. On the basis of the computed aerothermal loads, taking into account the effect of chemical non equilibrium, surface catalycity and emissivity, steady and time-dependent thermal analyses are necessary to demonstrate that the selected TPS is able to guarantee the structural integrity requirement and/or to update the initial design with suitable solutions.

Furthermore an optimization process has to be started to define an adjusted design for the crew launch configuration and especially the design of the mission depended resource module.

Also an evaluation of aerodynamic characteristics between 90 and 120 km in the rarefied regime seems to be necessary. This is mandatory, to evaluate the necessary corrections (in terms of Knudsen number) to the aero-database and to validate the aerocapture strategy at rarefied regimes.

A more detailed look to the environmental influences of the chemical non equilibrium effects and surface catalytic properties is required to guarantee the structural integrity requirements and/or to update the initial design with suitable solutions.

In the G&C workpackages of the study the necessity of implementation also the complete navigation functions were identified. For this the use of embedded GNSS (Global Navigation Satellite System) and IMU (Inertial Measurement Unit) navigation sensors shall be considered. Furthermore the computation of the black-out zone during re-entry shall be part of this continuative work, aiming at assessing the entry altitudes, where the GNSS signal can be properly received by the vehicle.

8 LITERATURE AND ABBREVIATIONS

8.1 APPLICAPLE DOCUMENTS

This document shall be read in conjunction with documents listed hereafter, which are applicable to this document to the extent specified therein. In case of a conflict between any provisions of this document and the provisions of the documents listed in Table 8-1, the content of the contractually higher document shall be considered as superseding.

Ref.-No.	Title and Issue, Author/Source/Website	Document No.	Organisation/ Publisher, Place & Date
[AD 1]	High Lift-over-Drag Earth Re-entry Strategies for Exploration Missions, Statement of Work, Issue final, Rev. 1	HMEHT/ RM/001.08	ESA/ESTEC, 30.01.2008
[AD 2]	Proposal to ESA for “High Lift-over-Drag Earth Re-entry Strategies for Exploration Missions”	Proposal Ref: OHB-1449-0108	OHB-System AG, 16/04/2008
[AD 3]	ECSS- E-10 Part 6A rev.1, 31, System engineering – Part 6: Functional and technical specifications		ESA October 2005

Table 8-1: List of applicable (normative) documents

8.2 REFERENCE DOCUMENTS

The following documents of Table 8-2 contain additional information that is relevant to the scope of this document.

Ref.-No.	Title and Issue, Author/Source/Website	Document No.	Organisation/ Publisher, Place & Date
TN 4.1		HL-GMV-TN-4.1_I1.2R1	OHB-Study-Team, 11.09.2008
TN 4.2		HL-GMV-TN-4.2-I1R0	OHB-Study-Team, 11.09.2008
TN 4.3		HL-OHB-TN-4.3 I2R0	OHB-Study-Team, 13.03.2009
TN 4.4-1		HL-OHB-TN-4.4-1_I1R0	OHB-Study-Team, 11.12.2008
TN 4.4-2		HL-GMV-TN-4.4-2_I2R0	OHB-Study-Team, 14.01.2009
TN 4.5		HL-DIAS-TN-4.5_I1R0	OHB-Study-Team, 17.04.2009,
TN 4.6		HL-OHB-TN-4.6_I1R0	OHB-Study-Team, 17.04.2009

Table 8-2: List of reference (informative) documents

8.3 ACRONYMS AND ABBREVIATIONS

Acronyms and Abbreviations	
AD	Applicable Document
AOCS	Attitude and Orbit Control Subsystem
AoA	Angle of attack
AoB	Angle of Bank
CEV	Crew Exploration Vehicle
CM	Command Module
DoF	Degree(s) of Freedom
EI	Entry Interface
ESA	European Space Agency
ESOC	European Space Operations Centre
ESTEC	European Space Technology Centre
FPA	Flight Path Angle
GNC	Guidance Navigation and Control
H/W	Hardware
I/F	Interface
LAS	Launch Abort System
LEO	Low Earth Orbit
L/D	Lift-over-Drag
LQR	Linear quadratic regulator
MRD	Mission Requirements Document
N/A	Not Applicable
P/L	Payload
PT	Product Tree
PHOEBUS	Plane-Shaped Hypersonic Orbital Re-Entry BUS
QA	Quality Assurance
RD	Reference Document
REV/Rev	Revision
S/S	Sub System
STS	Space Transportation System
SoC	Statement of Compliance
SOW	Statement of Work
SRD	System Requirements Document
TAEM	Terminal Area Energy Management
TAL	Transatlantic Abort Landing
TBC	to be confirmed
TBD	to be defined
TRL	Technology Readiness Level
NDI	Non Linear Dynamic Inversion
UHTC	Ultra High Temperature Ceramics
WBS	Work Breakdown Structure
WP	Work Package
WPD	Work Package Description
w.r.t	with respect to

Table 8-3: Acronyms and Abbreviations List